

## Chapter 6 Results - Old Head Model

Chapter 5 presented the results of the RP model. This model was used to determine the relative contributions of all of the outfalls, with the exception of Carrigaline/Crosshaven, to the contamination of the model oyster farm in the North Channel. This outfall was omitted from the RP model as it was positioned too close to the open boundary of the model at Roches Point. Viruses, which pass through the open boundary, are taken out of the model. For Carrigaline/Crosshaven this would lead to an unacceptable level of error in the *Norovirus* model. The Carrigaline/Crosshaven outfall has therefore been modelled using the Old Head (OH) model. The open boundaries of this model are approximately 12km from Roches Point.

### 6.1 The OH model

The OH model has four nested grids each with a different resolution (Fig. 6.1). The outer grid, from the Old Head of Kinsale to Roches Point is resolved with a 162m grid. The three grids nested within this area are identical to the three grids, which form the RP model. The OH model is therefore the RP model nested within an outer grid.

The parameters<sup>82</sup> of the RP model were used for the three inner grids of the OH model<sup>83</sup>. The hydrodynamic parameters of the 162m grid are listed on the next page. The advection dispersion parameters of the 162m grid were the same as for the other grids.

---

<sup>82</sup> Grid resolution, timestep, bed resistance, eddy viscosity, dispersion coefficient etc.

<sup>83</sup> The alterations to the open boundary of the RP model at Roches Point were not applied at the same location in the OH model. Adjustments were however made to the open boundaries of this model as can be seen from Fig. 6.1

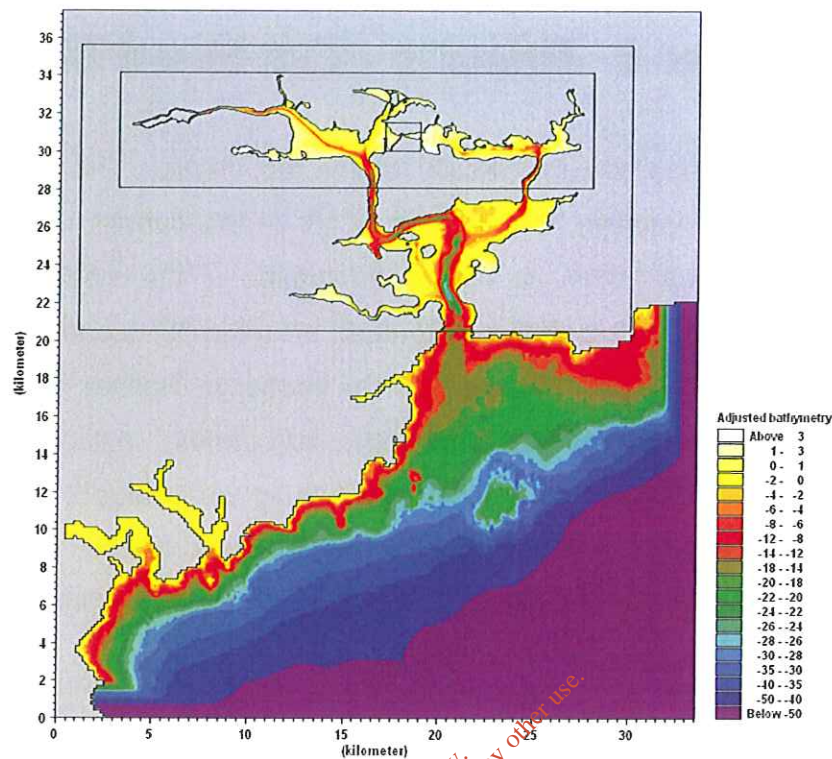


Fig. 6.1 Old Head (OH) model.

- **Eddy Viscosity** – A flux based eddy viscosity value of  $20\text{m}^2/\text{s}$  over the entire 162m grid was used. This value was reduced near Roches Point to agree with the value of  $1\text{m}^2/\text{s}$  used in the 54m grid.
- **Bed Resistance** – A Manning's M value of  $60\text{m}^{1/3}/\text{sec}$  over the entire 162 m grid was used.

## 6.2 Hydrodynamic Calibration

The boundary conditions of the OH model were provided by a numerical model, which covers part of the North West Atlantic Shelf. In other words the OH model is also embedded in a larger model. The Applications Group at the Proudman Oceanographic Laboratory (POL), UK, supplies hindcasts of (a) tide-plus-surge, and (b) tide-only levels on a grid covering part of the North Atlantic Shelf at frequencies of 1 hour for (a) and 20 minutes for (b) respectively. The centre uses its POL CS3 model to provide the annual hindcast at the end of each calendar year. Datasets are available from 1992 onwards.

Two years of hindcast data (1992 & 2004) were purchased from POL for this project. Data from the three points closest to the mouth of Cork Harbour, which form a right-angle, were selected from the CS3 grid and used to drive the hydrodynamics of the OH hydrodynamic model.

The tide-plus-surge data were interpolated between the data points and extrapolated between the data points and the land to form a profile series<sup>84</sup>. The two profile series describe the variation in water level and fluxes along the open boundaries of the model.

A period in June 2004 was selected from the two years of data to drive the hydrodynamic model<sup>85</sup>. This was the period in which the best calibration to the measured datasets was achieved. These datasets were provided by the Port of Cork and are the measurements of water level from the gauges at Cobh and Tivoli (Fig. 6.2).

The calibration plots for this period are highlighted in following figures<sup>86</sup>.

The calibration for a 60 hour period is shown in Fig. 6.3. We can see from the figure that the model is underestimating the water level by as much as 40cm. If we look at the entire period (Fig. 6.4) we can see that the maximum error varies between 28cm and 40cm.

The calibration plots for the gauge at Tivoli are shown in Fig. 6.5 (60 day period) and Fig. 6.6 (whole period). We can see from these plots that the error is slightly higher for Tivoli.

---

<sup>84</sup> A profile series contains data, which describes the variation in time of a variable along a line in space.

<sup>85</sup> The period in 1992 was not used for the OH model. The CS3 hindcast for 1992 was run with a meteorological model with a resolution of 50km. The output was not within an acceptable level of error. The 2004 hindcast used a meteorological model with a 12km resolution which significantly improved the accuracy of the CS3 model.

<sup>86</sup> Only water levels were calibrated. No current speed and direction measurements were available for this period.

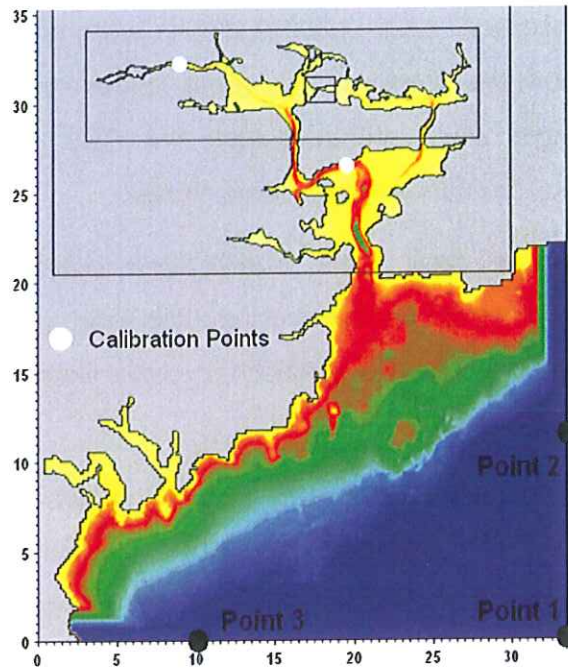


Fig. 6.2 Location of Calibration Points for the OH model

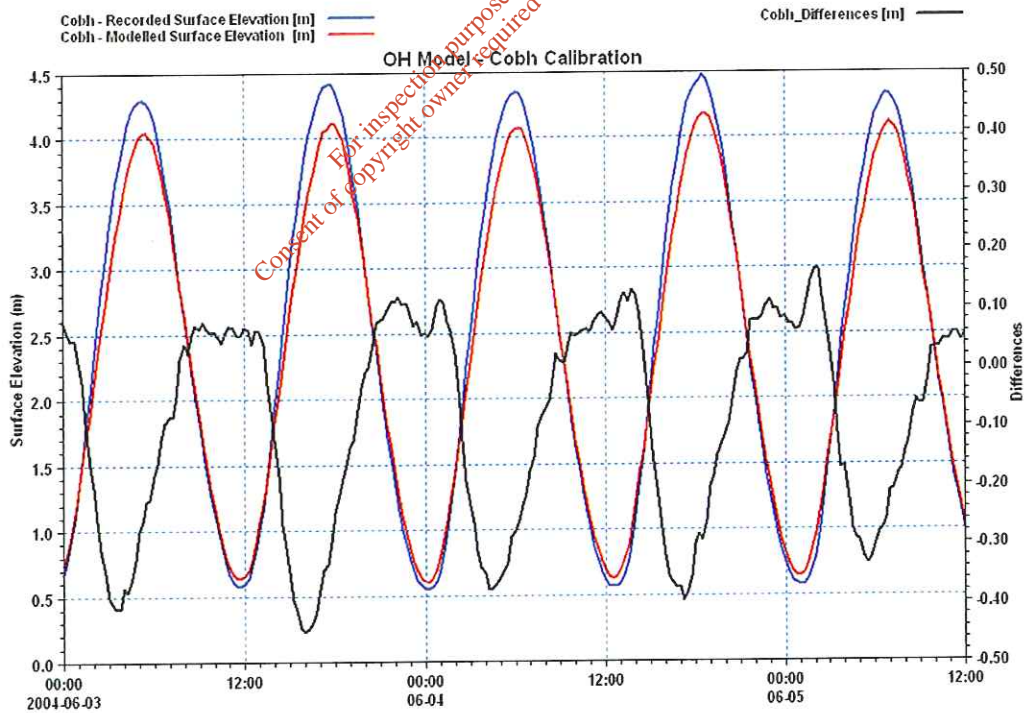


Fig. 6.3 Cobh Calibration for a 60 day period. The difference between the modelled and the measured is plotted using the black line on the second y-axis.

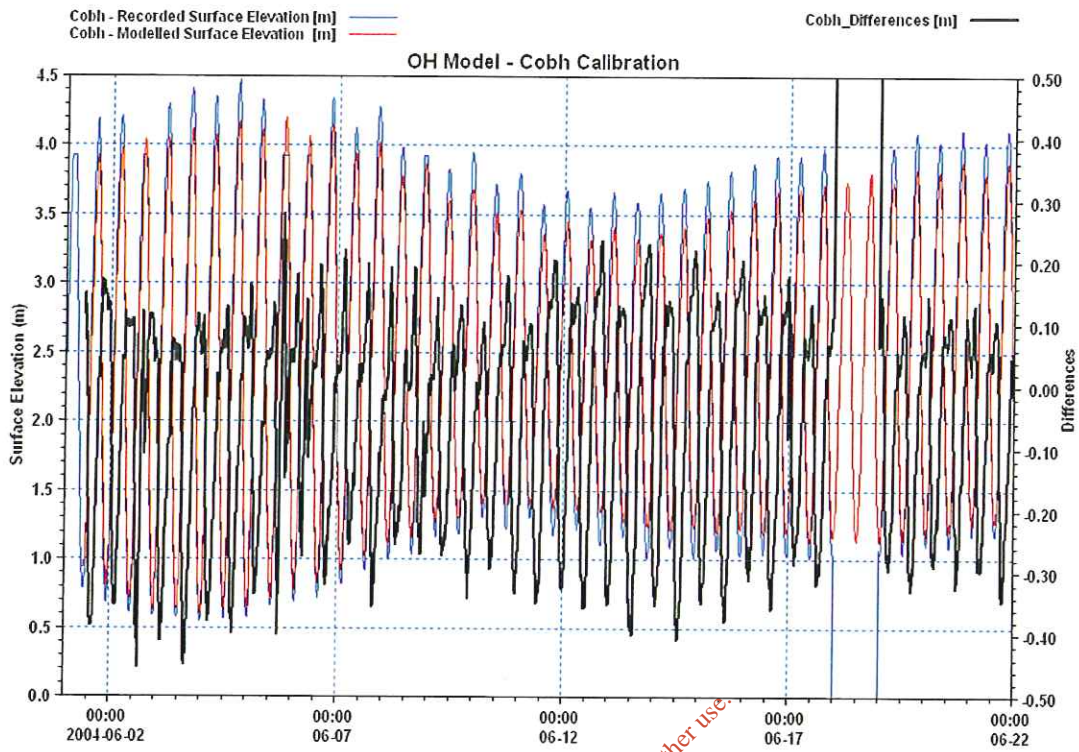


Fig. 6.4 Cobh Calibration for the entire period. We can see that the gauge failed on the 18<sup>th</sup> of June.

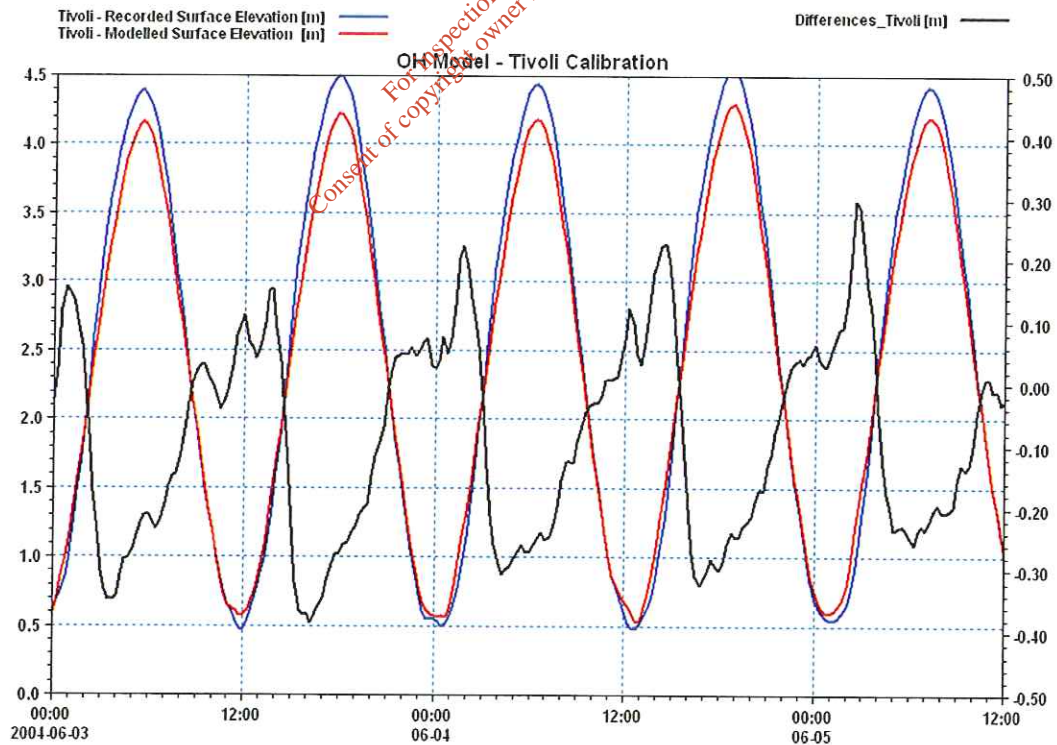


Fig. 6.5 Tivoli Calibration for a 60 day period. The difference between the modelled and the measured is plotted using the black line on the second y-axis.

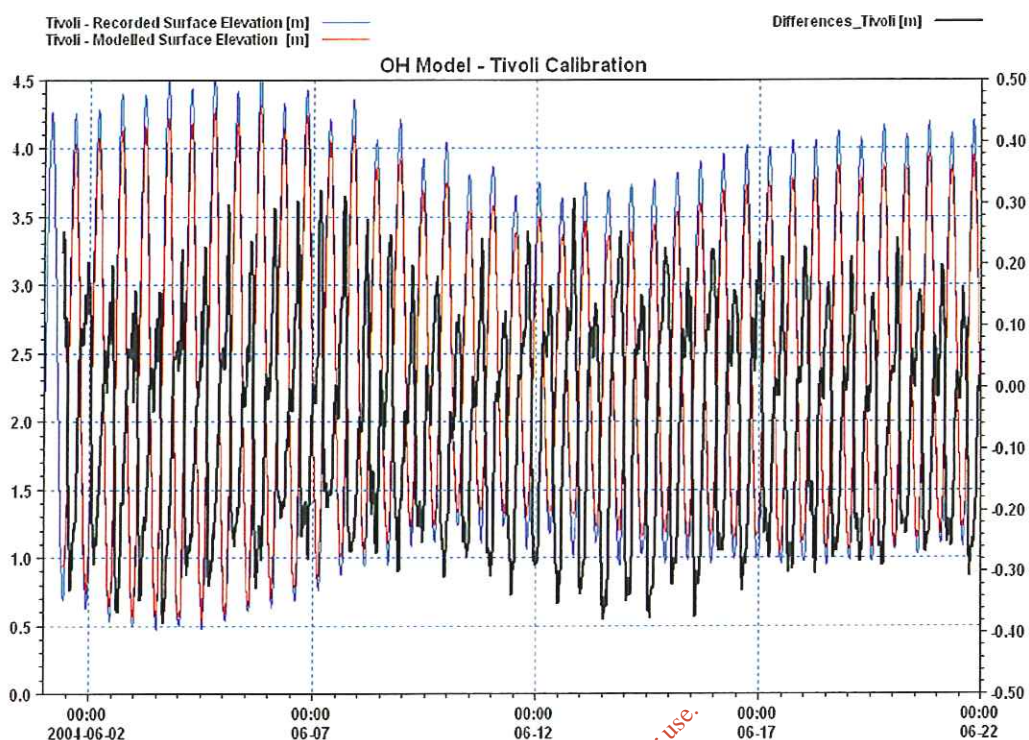


Fig. 6.6 Tivoli Calibration for the entire period.

The error associated with the Gobh and Tivoli gauges are not within an acceptable range<sup>87</sup>. An error of 40cm will lead to an unacceptable error in the tidal prism of the harbour, which in turn will lead to errors when modelling particles advected and dispersed by the tide.

Unlike the RP model, the boundary conditions of the OH model are not recorded measurements. They are outputs from a numerical model. Using one model to drive another has inherent limitations:

1. There is a potential for a cumulative build-up of errors. Any errors associated with the CS3 model will be propagated into the OH model. The open boundary of the CS3 model is the open sea along the North Atlantic shelf. The accurate description of this in the CS3 model could be a source of potential errors.

<sup>87</sup> Numerous other values of viscosity and bed resistance values were tried without success.

2. The resolution of the CS3 model is 12km. Therefore any data derived from it is representative of a 12km square water column in the Celtic Sea.
3. There was no downscaling from the 12km grid of the CS3 to the 162 m outer grid of the OH model i.e. no intermediate grid. Overcoming this particular problem would have required purchasing additional data for points further out in the Celtic sea.

When these limitations are considered we can see that the calibration of the OH model is reasonably good. It is not good enough however to replace the RP model.

The main objective in using the OH model is to determine the relative contribution of Carrigaline and Crosshaven to the contamination of the oyster farm. We can do this by comparing the contribution of Carrigaline/Crosshaven with the contribution of the other outfalls simulated using the OH model. We cannot make direct comparisons with results obtained from the RP model<sup>88</sup>.

A comparison between Carrigaline and Crosshaven with Cobh, Midleton and Cloyne for summer and winter conditions is presented in the following two sections. These outfalls have been chosen as they are the ones which lie closest to the oyster farm. The error associated with them is therefore less than for ones further away.

### 6.3 Summer Conditions

The summer conditions presented in this section used the recorded wind and river flows from June 2004. This corresponded to a period of exceptionally low flows in the River Lee and Owenacurra<sup>89</sup>.

---

<sup>88</sup> As well as the error in the OH model, the boundary conditions are for a different period than that used for the RP model (i.e. there is a different tidal signal in the harbour and so a like-for-like comparison is not possible).

<sup>89</sup> The flows in rivers were so low that they were selected for the sensitivity analysis in Chapter 8.

The timeseries of concentration for Carrig and Cobh\_R are plotted in Fig. 6.7. The moving averages are plotted in Fig. 6.8. We can see from both figures that Carrigaline\_C is contributing less than Cobh\_R for the 20 days shown. We can see that the peaks in concentration from Cobh are up to 4 times larger than the peaks from Carrigaline\_C. We can also see that there is a factor of two to three difference in the averages.

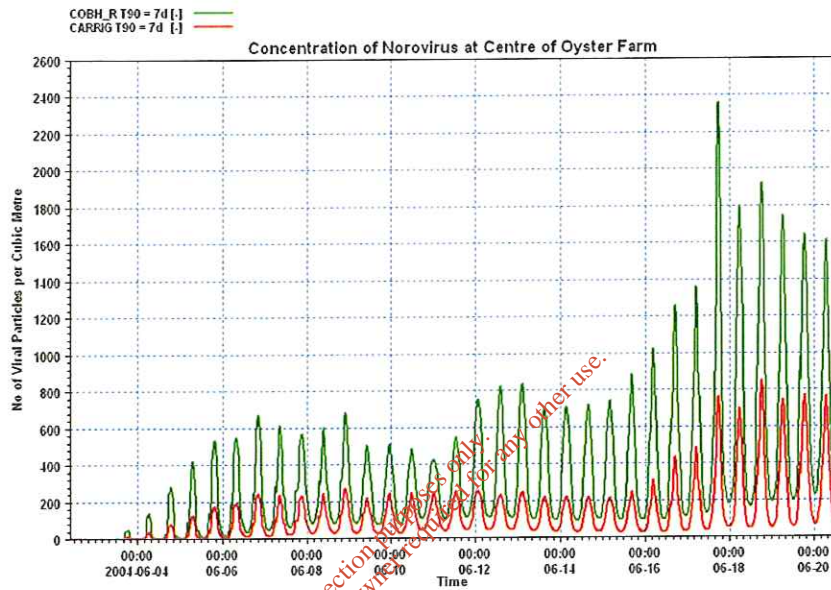


Fig. 6.7 Timeseries of Carrigaline/ Crosshaven and Cobh\_R at Centre of Oyster Farm – Summer Conditions

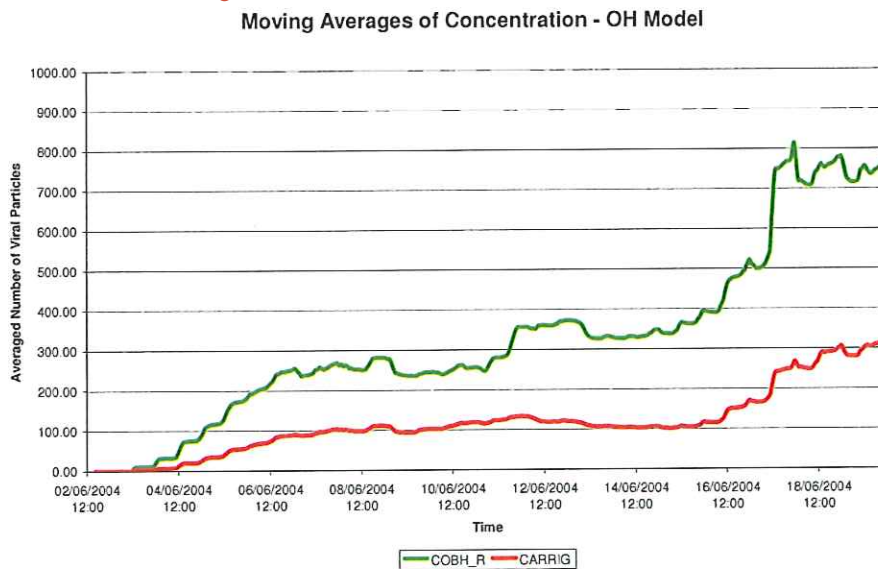


Fig. 6.8 Moving Averages for Cobh and Carrigaline\_C



Carrigaline\_C is plotted against Cloyne and the untreated waste from Midleton in Fig. 6.9 and Fig. 6.10. We can see that Cloyne is contributing more initially but by the end of the simulation they are contributing an equal amount. The untreated waste from Rathcoursey is contributing much more than Carrigaline\_C.

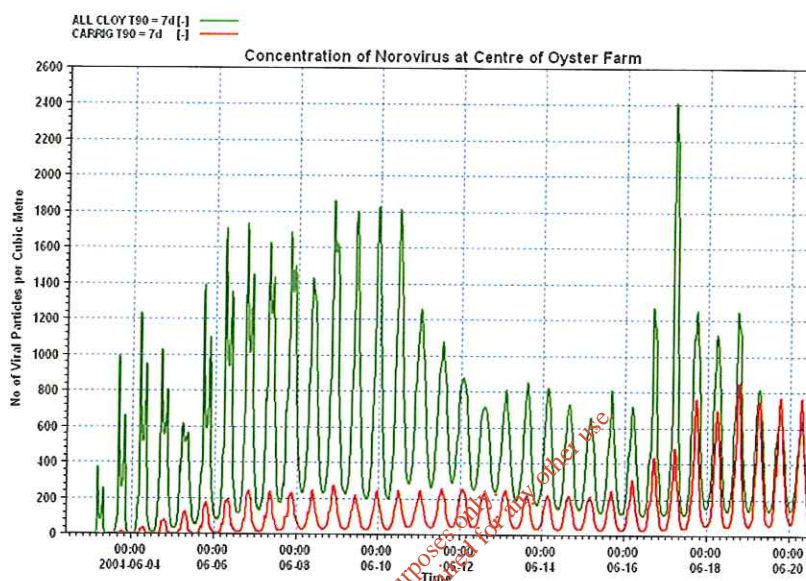


Fig. 6.9 Timeseries of Carrigaline/ Crosshaven and ALL\_CLOYNE at Centre of Oyster Farm – Summer Conditions

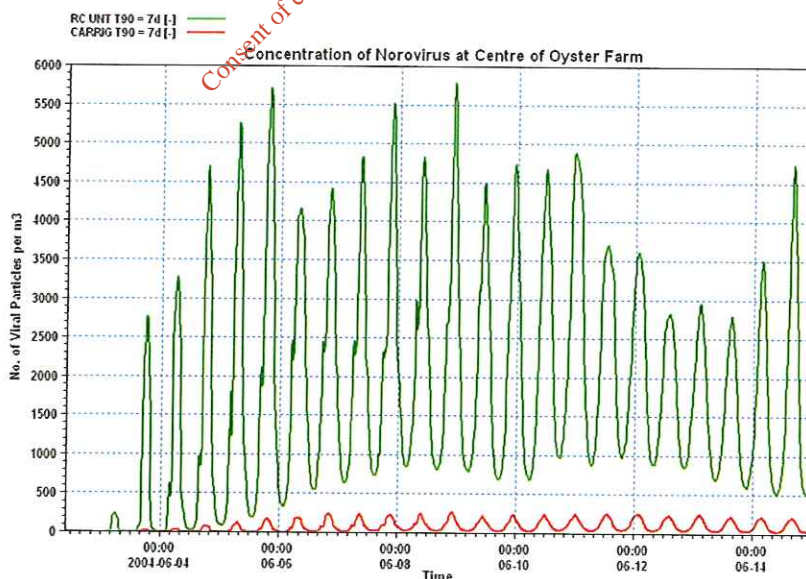


Fig. 6.10 Timeseries of Carrigaline/ Crosshaven and RC\_S&C at Centre of Oyster Farm – Summer Conditions

## 6.4 Winter conditions

The winter conditions were simulated using the wind and river flows from the 1992 dataset used for the RP model runs to simulate more realistic winter conditions.

The time series of concentration for Carrigaline\_C and Cobh\_R are plotted in Fig. 6.11 for winter conditions. We can see from the figure that the relative contribution for the outfalls has changed slightly. Relative to Cobh\_R, Carrigaline\_C is contributing less than half that of Cobh. With the slower decay in winter months the greater distance of Carrigaline\_C to the oyster farm becomes less relevant. This is also evident for Fig. 6.13 where we can see Carrigaline\_C plotted with the untreated waste from Midleton. While Midleton is contributing more than Carrigaline\_C the difference between the two is less, relatively speaking, than for the summer conditions.

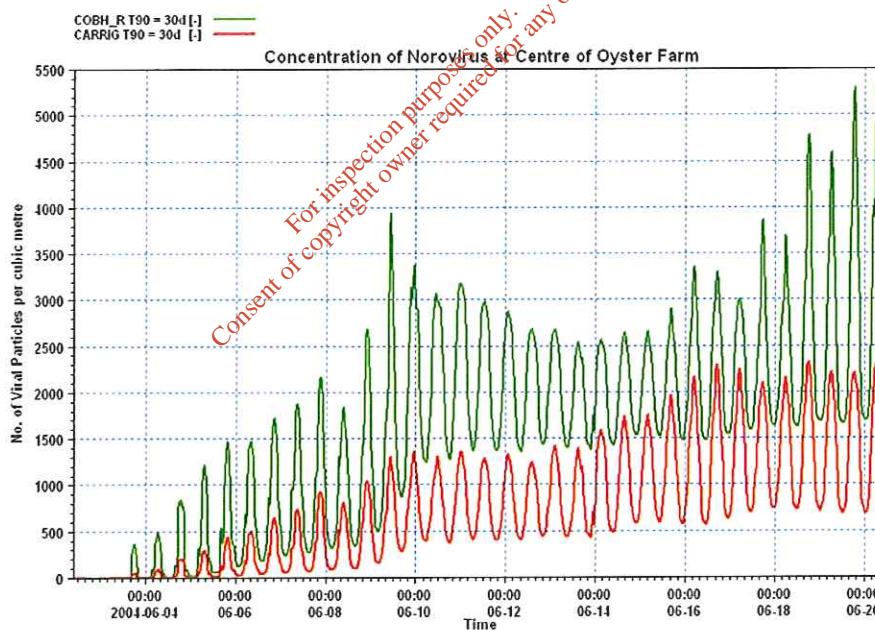


Fig. 6.11 Timeseries of Carrigaline/ Crosshaven and COBH\_R at Centre of Oyster Farm – Winter Conditions

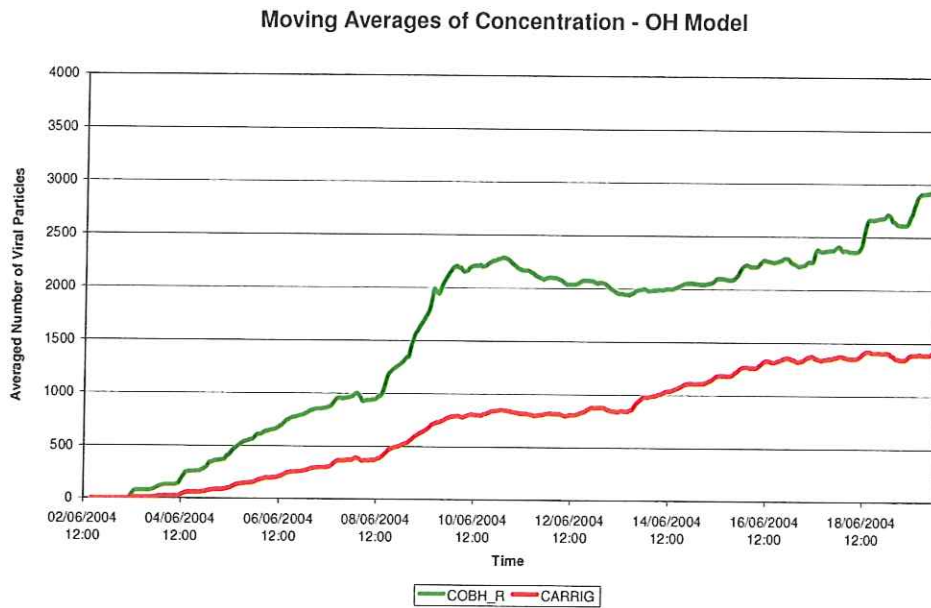


Fig. 6.12 Moving Averages for Cobh\_R and Carrigaline\_C – Winter Conditions

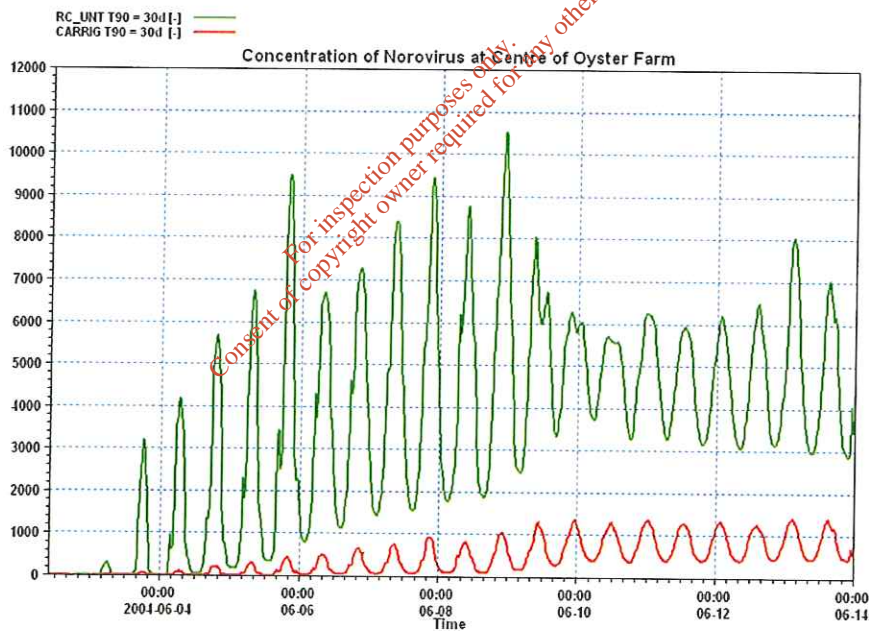


Fig. 6.13 Timeseries of Carrigaline/ Crosshaven and RC\_S&C at Centre of Oyster Farm – Winter Conditions

## **6.5 Conclusions**

The release of viral particles from the combined outfall for the towns of Carrigaline and Crosshaven has been simulated using the Old Head model. A direct comparison with the RP model is not possible.

The results presented in the chapter indicate that for summer conditions the contribution of Carrigaline and Crosshaven is approximately a third of the contribution of Cobh and Ringaskiddy. In winter it is approximately half.

*For inspection purposes only.  
Consent of copyright owner required for any other use.*

## Chapter 7 Sensitivity Analysis

### 7.1 Introduction

A sensitivity analysis has been undertaken as part of the study. The purpose of a sensitivity analysis is to identify which uncertainties in the model may or may not alter significantly the results of the model.

A number of the parameters used in the models have been adjusted and are presented in this Chapter. The sensitivities presented are:

1. Assume 20 million viral particles per cubic metre in raw sewage. Assume an 85% removal efficiency from a secondary waste water treatment plant
2. Apply a different numerical scheme (ULTIMATE) to the *Norovirus* model.
3. Specify the dispersion coefficient as (a) proportional to the current, and (b) a function of the grid spacing and timestep (independent of the current)
4. Run the model without any wind forcing.
5. Run the summer conditions with extremely low river flows but with the same wind forcing as in Chapter 5.
6. Divide the untreated waste from Cork City (before Carrigrennan was constructed) between the City, Tramore and Little Island outfalls.
7. Include Salinity in the hydrodynamic model.
8. Examine different release patterns from Rathcoursey and make a direct comparison between releasing *Norovirus* at Rathcoursey and Bailick road in Midleton.
9. Consider adsorption of *Norovirus* on Suspended Sediment.

### 7.2 Sensitivity One

In the results presented in Chapter 5 we have assumed 50 million *Norovirus* are

present in every cubic metre of raw sewage. We have also assumed that 95% of the *Norovirus* are removed in a secondary waste water treatment plant (discussed in Appendix D). A similar study to ours undertaken by a team of microbiologists at IFREMER<sup>90</sup>, France, assumed that (a) there are 20 million *Norovirus* present in every cubic metre of raw sewage and (b) the removal efficiency of secondary treatment is 85%. We have scaled our timeseries of concentration at the centre of the oyster farm as presented in Chapter 5 to match these assumptions.

If we rescale the results by just considering the first assumption on its own we find that the relative contributions are unchanged for each of the six cases. This is to be expected as the reduced number of *Norovirus* per cubic metre is applied to each and every outfall and so the concentration at the centre of the model oyster farm is reduced by 60% for the entire simulation period.

When we rescale the results considering both assumptions we find that the relative contributions for some of the cases change. For the first two cases (Period 1, summer and winter) the relative contributions do not change as there are no treatment plants in operation during this period and the reduction in the number of *Norovirus* is applied to each outfall.

For the cases 3 and 4 (Period 2, summer and winter) there is a very minor change to the relative contributions. This is due to an increase in the contribution of the treated waste from Rathcoursey as it is now assumed to be removing 85% of the *Norovirus*. This difference however is approximately 1% reflecting the minor contribution of RC\_S&C.

When the results for Case five and Case six are rescaled we find a significant difference in the relative contributions. The removal efficiency of Carrigrennan and Rathcoursey is now reduced from 95% to 85% and so both are contributing

---

<sup>90</sup> Pommepuy, M. et al. "Fecal contamination in coastal waters: An engineering approach" Book chapter (p331-359) in *Oceans and Health: Pathogens in the Marine Environment*. Springer 2006. <http://www.springerlink.com>, <http://www.ifremer.fr/docelec>

a greater number of viral particles to the oyster farm. The storm water overflows, the houses and Cobh etc are all contributing less.

The relative contributions for the rescaled Case 5 are presented in Fig. 7.1. To aid the reader in making a comparison the relative contributions for Case 5, as presented in Chapter 5, is repeated underneath in Fig. 7.2.

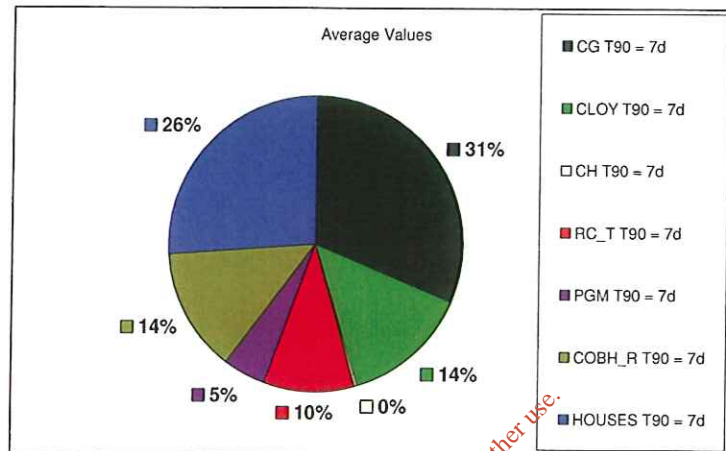


Fig. 7.1 CASE 5 – Average Concentrations – The Relative Contributions **after** rescaling

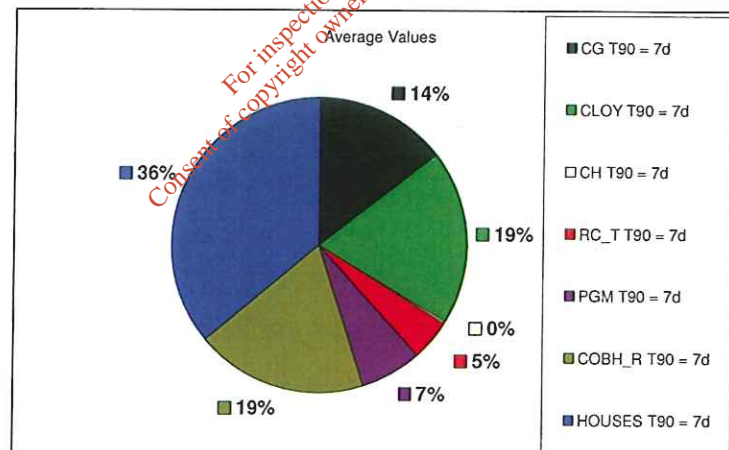


Fig. 7.2 CASE 5 – as presented in Chapter 5

We can see from the figures that Carrigrennan is now contributing more than the Houses around the North Channel. Cobh and Cloyne are contributing less than before.

The relative contributions for the rescaled Case 6 are presented in Fig. 7.3. The relative contributions for Case 6, as presented in Chapter 5, are repeated underneath in Fig. 7.4.

We can see from the figures that Carrigrennan is contributing as much as the overflows from Baillick 1.

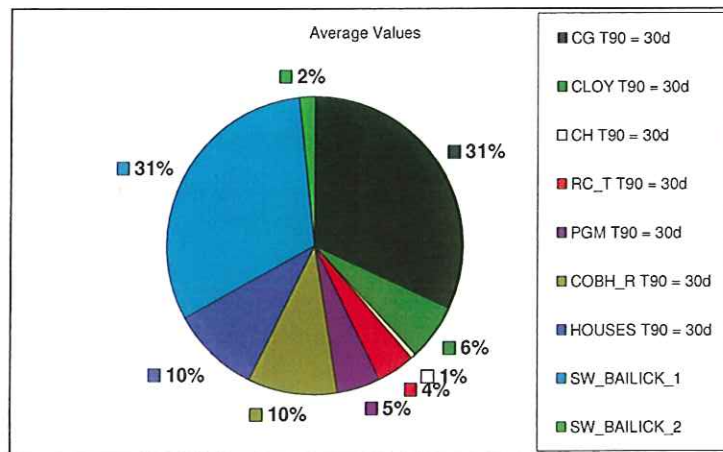


Fig. 7.3 CASE 6 - Average Concentrations – The Relative Contributions **after** rescaling

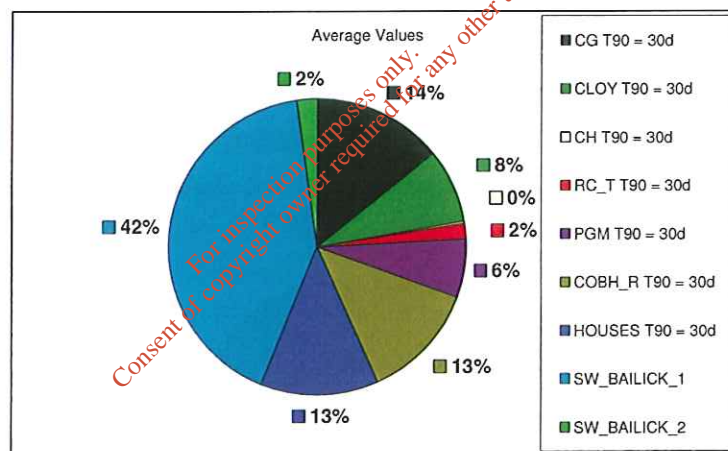


Fig. 7.4 Case 6 – Average Concentrations – as presented in Chapter 5

From these plots we can see that the relative contribution of Carrigrennan to the contamination of the model oyster farm is very sensitive to its removal efficiency. By assuming a reduction in removal efficiency from 95% to 85% the relative contamination increases from 14% to 31%.

### 7.3 Sensitivity Two – ULTIMATE scheme, Winter Conditions

There are four numerical schemes in MIKE 21 which may be used to simulate the advection and dispersion of *Norovirus* in Cork Harbour. These schemes are:



- The Quickest Scheme<sup>91</sup>
- The ULTIMATE scheme<sup>92</sup>
- Simple UPWIND
- 2D UPWIND

The results presented in Chapter 5 used the Quickest scheme. As part of the sensitivity analysis we have simulated a number of the outfalls using the ULTIMATE scheme. The UPWIND schemes were not used.

The following three figures present both the Quickest and ULTIMATE timeseries of concentrations for three of the sources of *Norovirus* in our study. We can see from the figures that the differences between the two schemes are very minor. The Quickest scheme gives slightly higher peaks in concentration for each of the sources. From this we can conclude that there is very little difference between the Quickest or ULTIMATE schemes for the simulation of *Norovirus* in Cork Harbour.

For inspection purposes only  
Consent of copyright owner required for any other use.

---

<sup>91</sup> Ekebjærg, L. (1991), " An explicit scheme for advection-diffusion modelling in two dimensions", *Computer Methods in Applied Mechanics and Engineering*, 88, pp. 287-297

<sup>92</sup> Leonard, B.P. (1991), " The ULTIMATE conservative difference scheme applied to one-dimensional advection", *Computer Methods in Applied Mechanics and Engineering*, 19, pp. 59-98

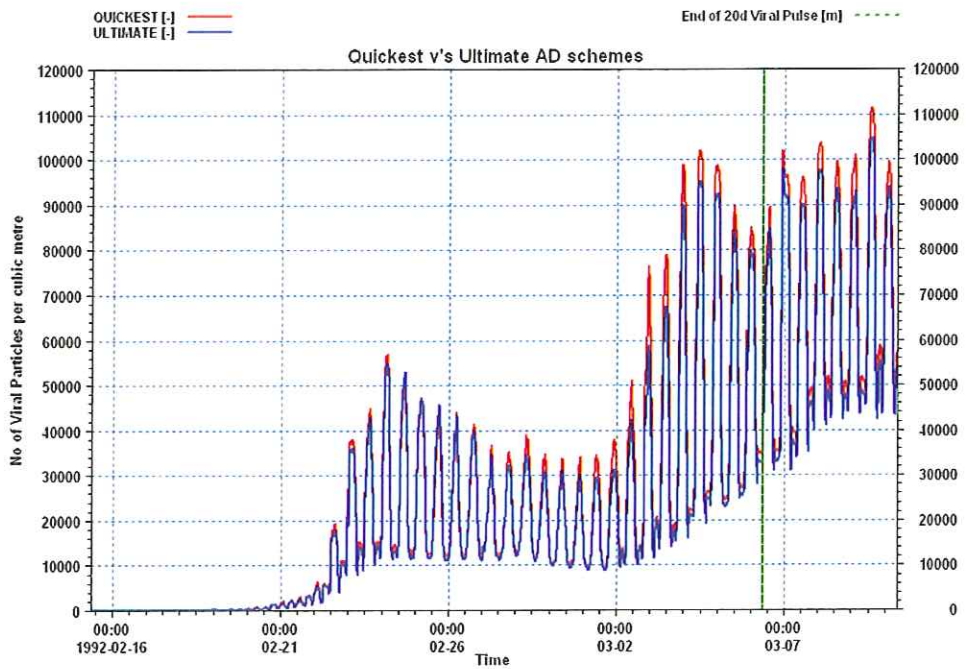


Fig. 7.5 CC\_S&C – ULTIMATE and Quickest Schemes

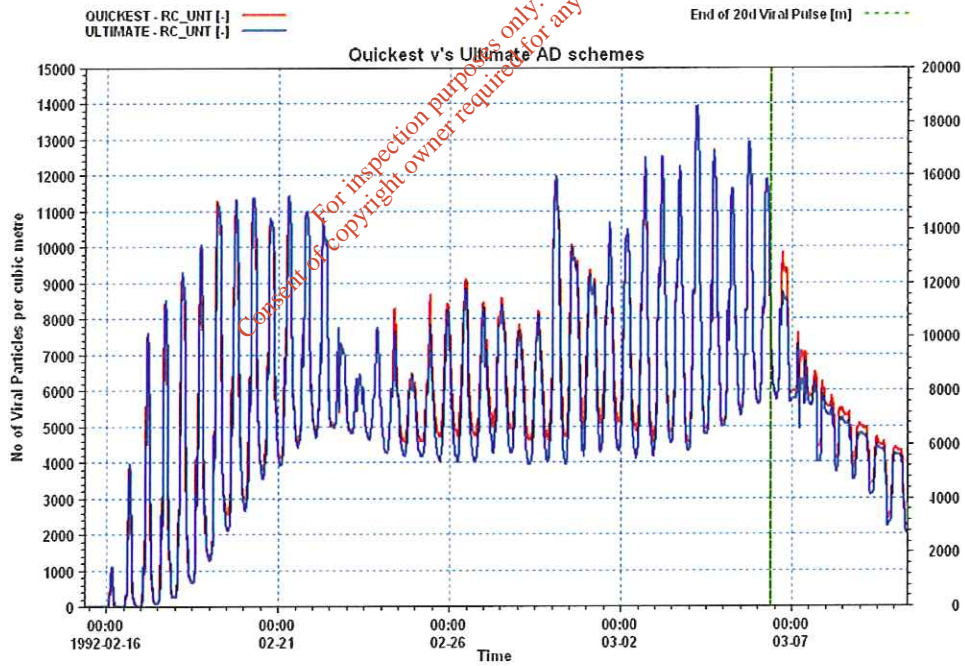


Fig. 7.6 RC\_S&C ULTIMATE and Quickest Schemes

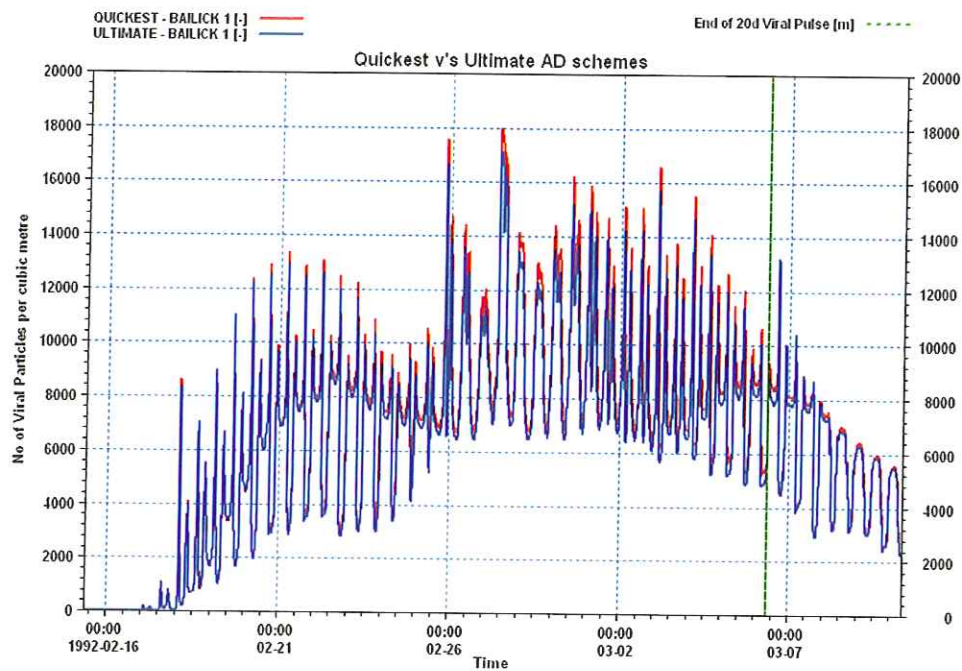


Fig. 7.7 Comparison of Overflows from Bailick 1 using the Quickest and ULTIMATE schemes

## 7.4 Sensitivity Three – Dispersion Coefficient, Winter Conditions

Two separate sensitivities are examined in relation to the dispersion coefficient. The first specifies the coefficient as proportional to the current while the second uses a very high value independent to the current option.

### 7.4.1 Proportional to the current

There are two ways in which to define the dispersion coefficient in MIKE 21:

- Independent of the current
- Proportional to the current

The results presented in Chapter 5 used the “independent of the current” option. A constant value of  $1\text{m}^2/\text{s}$  was used over the entire grid in both the x- and y-directions. As part of the sensitivity analysis the “proportional to the current” option was used. When this option is chosen the dispersion coefficients are, at every timestep, scaled in accordance with the calculated fluxes. Maximum and

minimum values are defined to avoid instabilities. A proportionality factor for each direction is also defined.

The values used in the sensitivity were:

Minimum Value =  $0.3\text{m}^2/\text{s}$ ; Maximum Value =  $2\text{m}^2/\text{s}$ ; Proportional Factor in x- and y- direction = 1

The maximum value was set at  $2\text{m}^2/\text{s}$  to avoid numerical instabilities in the *Norovirus* model.

The differences between the two different options are presented in Fig. 7.8 for CC\_S&C and Fig. 7.9 for RC\_S&C. We can see from both figures that the differences between the different options are negligible.

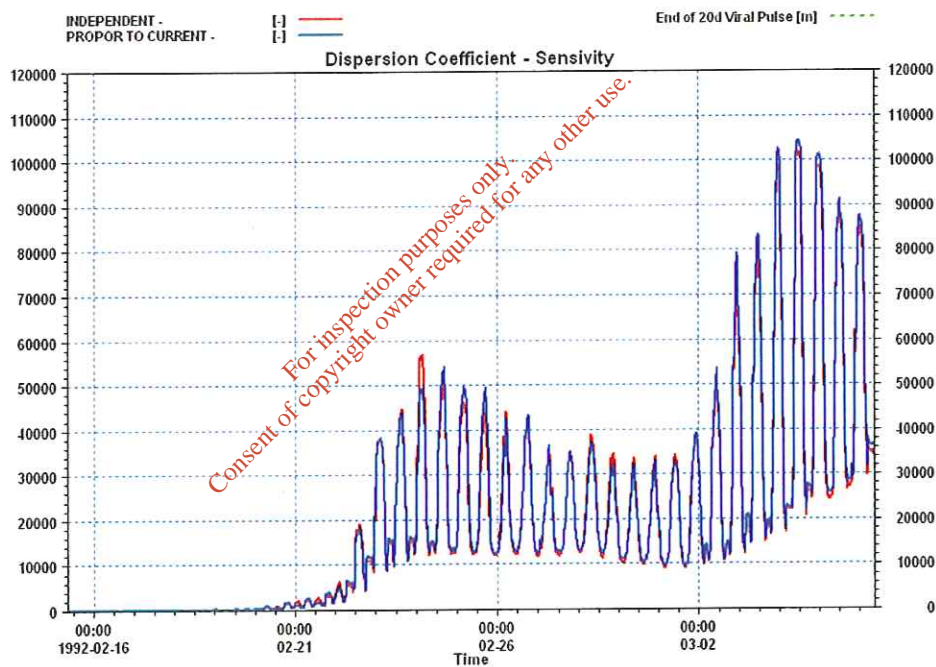


Fig. 7.8 Dispersion Coefficient Sensivity – CC\_S&C

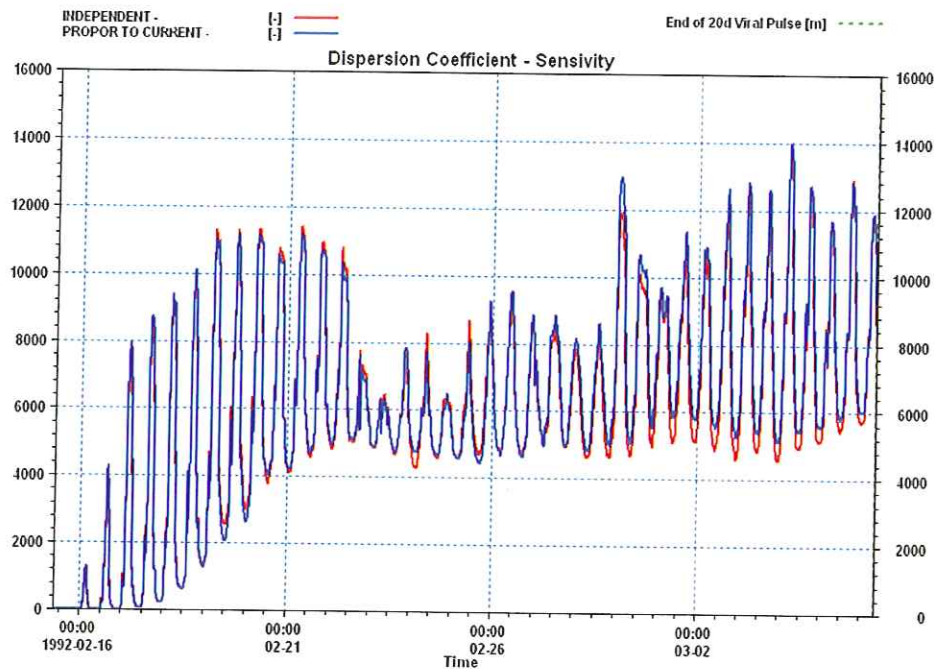


Fig. 7.9 Dispersion Coefficient Sensivity – RC\_S&C

#### 7.4.2 “Independent of the Current” – Coefficients as a function of the grid spacing and timestep

The results presented in Chapter 5 used  $1\text{m}^2/\text{s}$  as the value for the dispersion coefficient. This value was constant across each of the nested grids and was defined as being “independent of the current”. As part of the sensitivity analysis the dispersion coefficient was specified as a function of the grid spacing and timestep through the formula:

$$D_x = K \{ \Delta x^2 / \Delta t \}$$

where

- $D_x$  is the dispersion coefficient
- $K$  is a dimensionless empirical constant
- $\Delta x$  is the grid spacing
- $\Delta t$  is the timestep

A value of  $1\text{m}^2/\text{s}$  is required for the 6m grid to ensure numerical stability (implying that  $K$  is approximately 0.1). From this formula we find:

- $D_x = 0.9\text{ m}^2/\text{s}$  for the 6m grid;
- $D_x = 8.1\text{ m}^2/\text{s}$  for the 18m grid;
- $D_x = 72.4\text{ m}^2/\text{s}$  for the 54m grid;

Using these values as a guide we have defined a grid based dispersion coefficient map as part of this sensitivity analysis (Fig. 7.10). We can see from the plot that the 6m grid has a value of  $1\text{ m}^2/\text{s}$ ; the 18m grid has a value of  $10\text{m}^2/\text{s}$  and the 54m grid has a value of  $50\text{m}^2/\text{sec}$ .

These values are extremely high and represent the upper limit of realistic values of the dispersion coefficient. If they were applied to the eddy viscosity in the hydrodynamic model the current speed and direction calibration for Lough Mahon and the Spit Bank as presented in Chapter 3 would not be as good. The eddies which form in the outer harbour would also be significantly reduced contrary to the observation of harbour pilots and sailors.

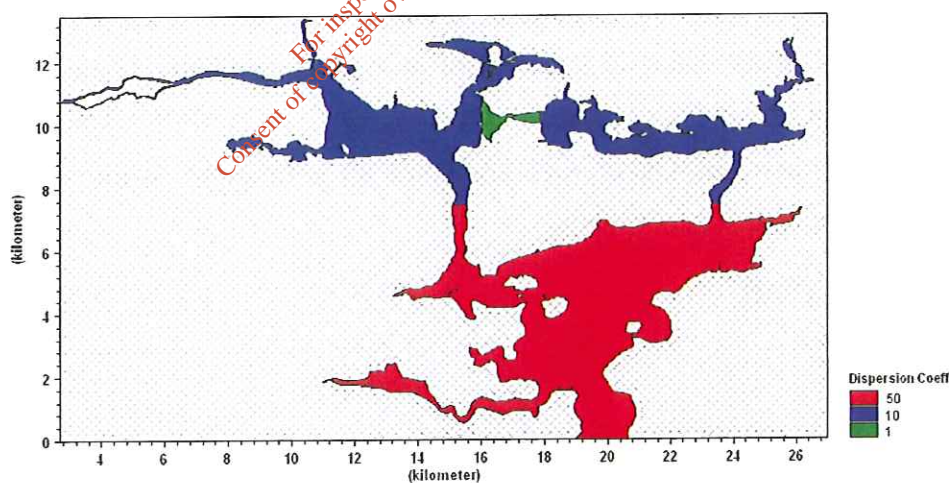


Fig. 7.10 Dispersion Coefficient Map

The timeseries of *Norovirus* concentration for sensitivity analysis are now presented. We can see from Fig. 7.11 that with the higher dispersion coefficients the contribution from CC\_S&C is marginally higher. The peak values in concentration are consistently higher by 20 – 30%.

We can see from Fig. 7.12 that the contributions from Cobh\_R for both cases are very similar with the exception of the period after the strong wind from the west on the 23<sup>rd</sup> of February. For this period the peak values in contamination are reduced due to the enhanced dispersion in the outer harbour.

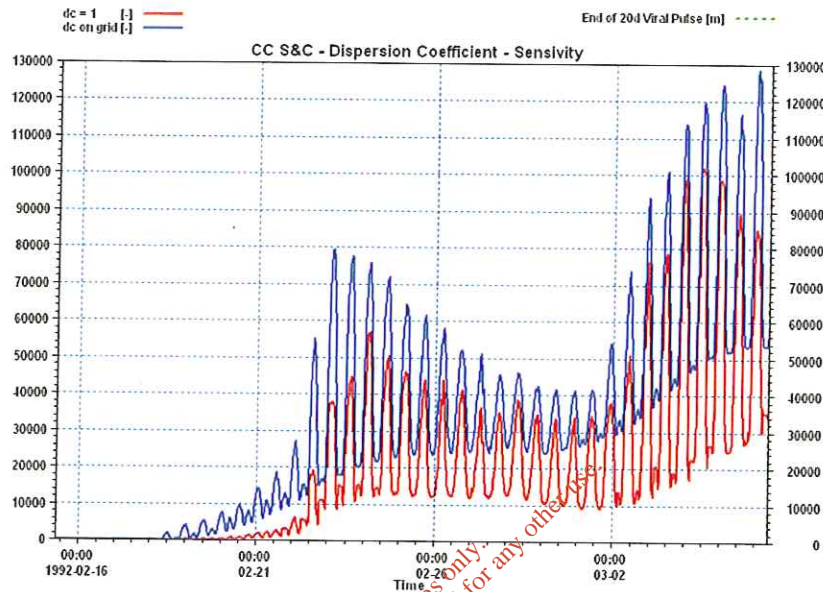


Fig. 7.11 CC\_S&C dispersion coefficient sensitivity

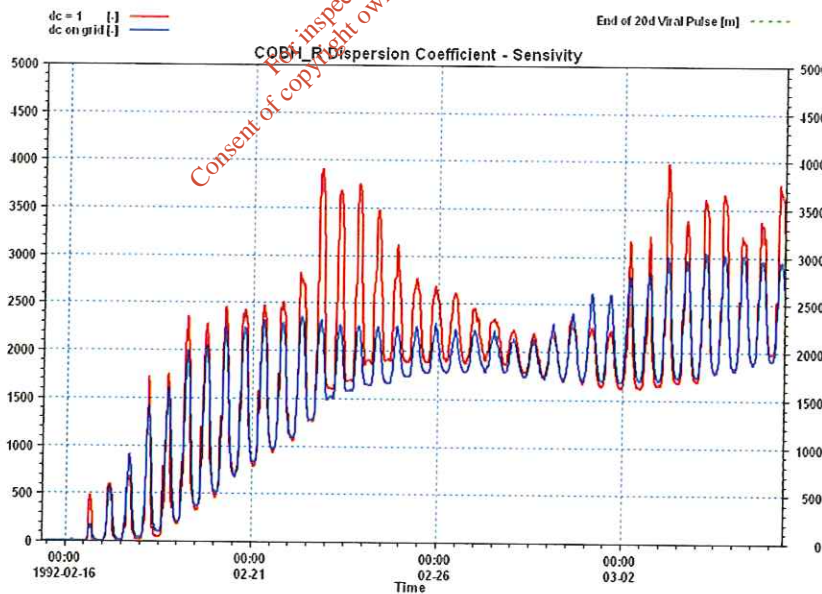


Fig. 7.12 Cobh\_R dispersion coefficient sensitivity

From Fig. 7.13 we can see that the contribution from RC\_S&C is reduced with the higher dispersion coefficients.

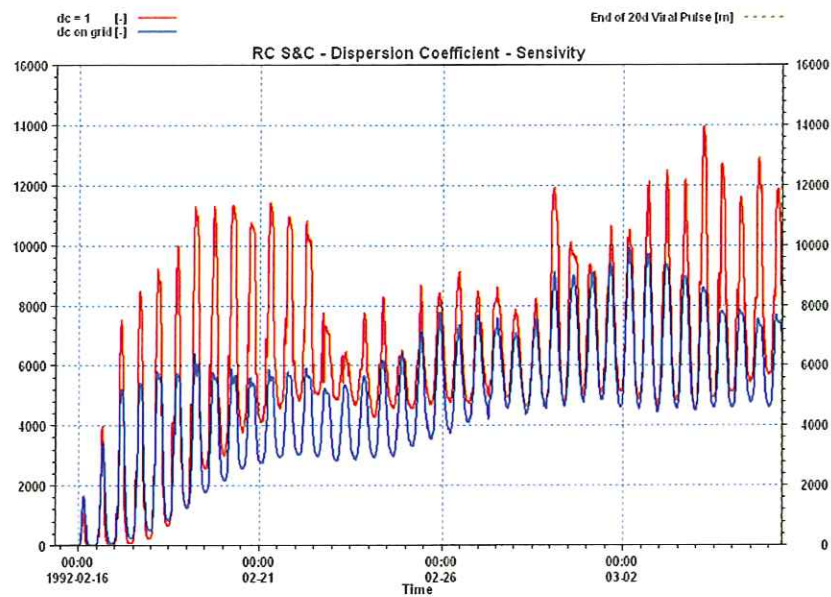


Fig. 7.13 RC\_S&C dispersion coefficient sensitivity

## 7.5 Sensitivity Four – No wind, Winter Conditions

The influence which the wind exerts was described in Chapter 5. As part of the sensitivity analysis we have run a simulation in which the wind was omitted. For this simulation the same river flows as before were used.

Fig. 7.14 presents the timeseries of concentration for the untreated sewage from Cork at the centre of the model oyster farm for winter conditions. We can see that the contribution is much less when the wind is omitted. With no wind blowing the number of viral particles passing through the Belvelly Channel is greatly reduced. This has a considerable influence on the relative contribution of CC\_S&C (and CG) on the contamination of the model oyster farm. The moving averages of concentration are presented in Fig. 7.15. We can see from the figure that including the wind approximately doubles the contribution of CC\_S&C. If we plot the tidal signal from Fort Camden with the extracted timeseries for a short period (Fig. 7.16) an interesting pattern emerges. We can see from the figure that when the wind is included the concentrations rise to a maximum on the ebb tide. When the wind is excluded the concentrations rise on the flood tide. This clearly illustrates that wind plays a significant role in contaminating the model oyster farm. The peak in concentration on the ebb tide indicates that the viruses



are passing through the Belvelly Channel on the preceding flood tide and are carried through the model oyster farm on the ebb tide. When the wind is excluded the main route by which the viruses are carried to the model oyster farm is around Cobh Island. In this case the peak in concentration occurs on the flood tide as the water from the outer harbour, carrying all the viruses, flows up the East Passage and into the North Channel.

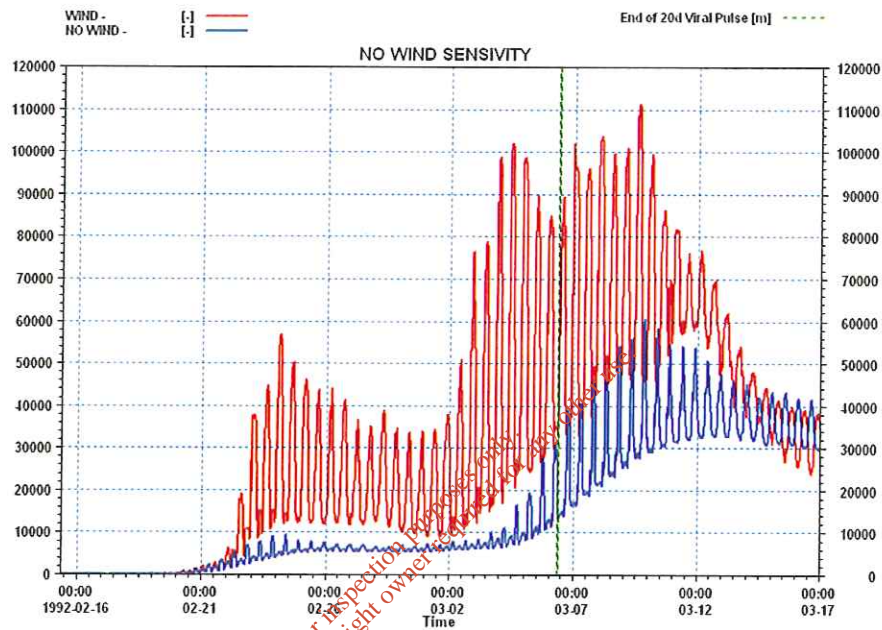


Fig. 7.14 No Wind Forcing Sensitivity – CC\_S&C

Untreated Waste, Cork City - Moving Averages of Concentration

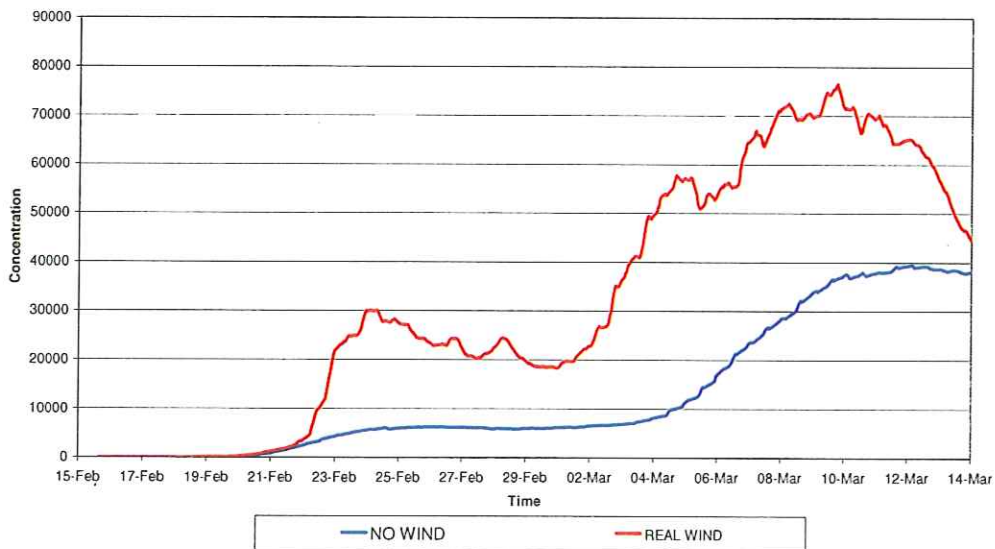


Fig. 7.15 Moving Averages of Concentration for the CC\_S&C – Wind Sensitivity

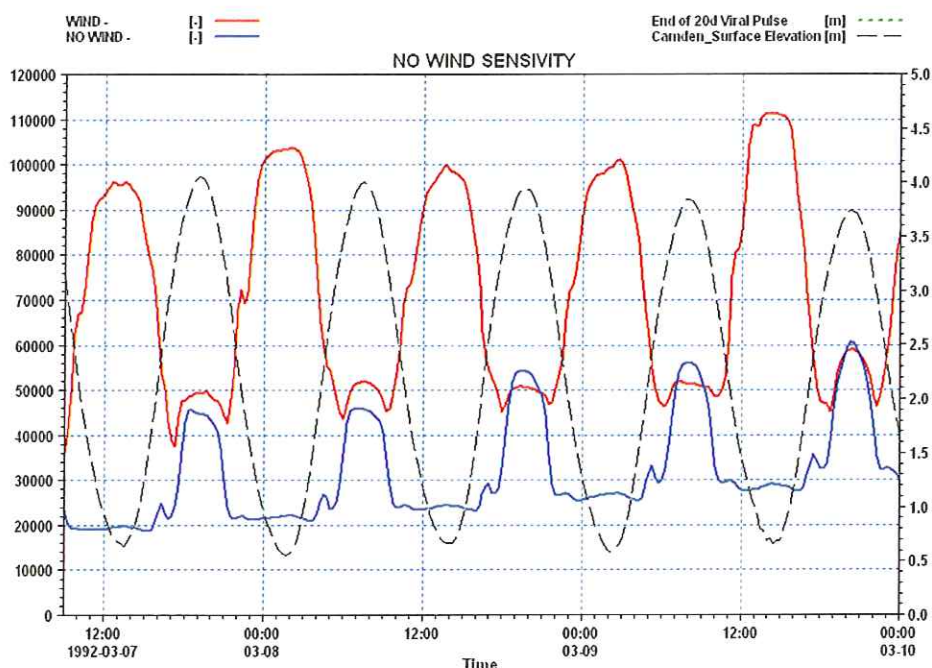


Fig. 7.16 No Wind Sensitivity with Tidal Signal - Close up view. The tidal signal is plotted using the dashed black line on the secondary y-axis.

From Fig. 7.17 we can see that the opposite is the case for RC\_S&C. With no wind blowing the contribution is increased. This result is to be expected. The winds from the West and South West which increase the contribution of CC\_S&C decrease the contribution of RC\_S&C such that when the wind is removed the contribution increases. The moving averages are plotted in (Fig. 7.18). We can see from the figure that the averaged concentrations only start to diverge when the strong wind from the west blows on the 22<sup>nd</sup> of February. They diverge further when the wind blows from this direction again in a later period at the start of March.

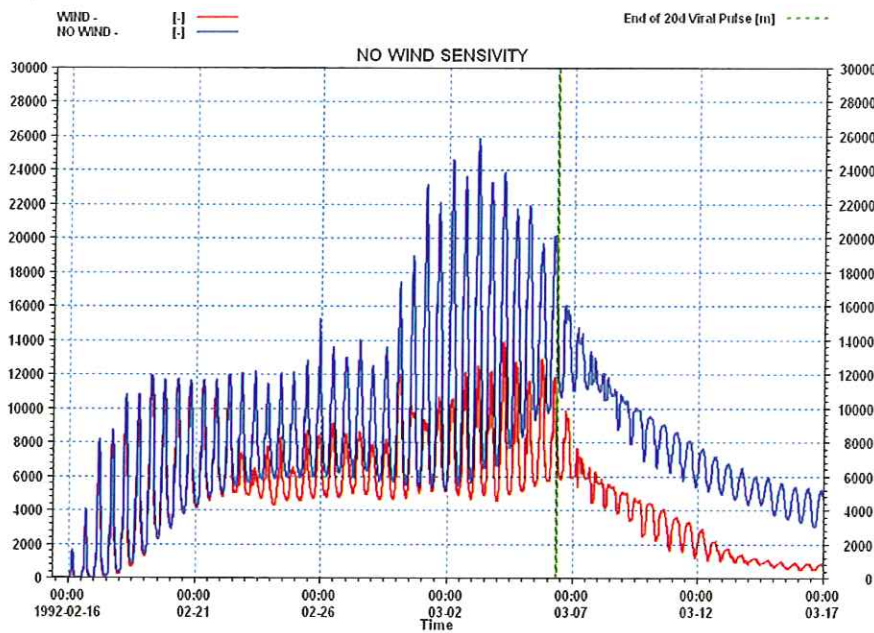


Fig. 7.17 No Wind Forcing Sensitivity – RC\_S&C

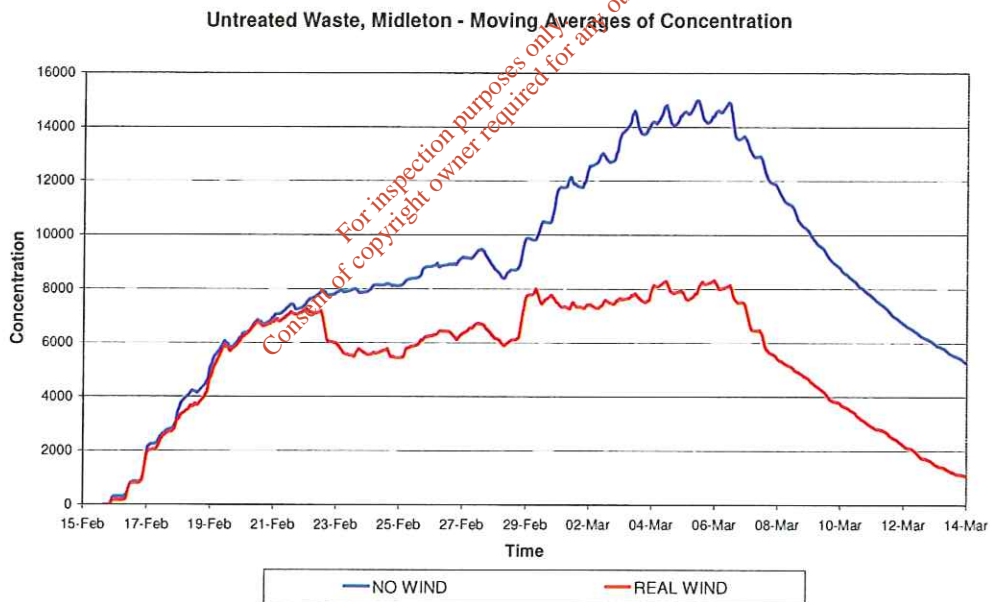


Fig. 7.18 Moving averages of concentration for RC\_S&C

From Fig. 7.19 we can see that the influence which wind exerts on the contribution of COBH\_R to the model oyster farm also varies. For the first 20 days the concentrations are consistently higher by a relatively small amount. After strong winds from the South around the 5<sup>th</sup> of March the contribution drops with the real wind simulation.

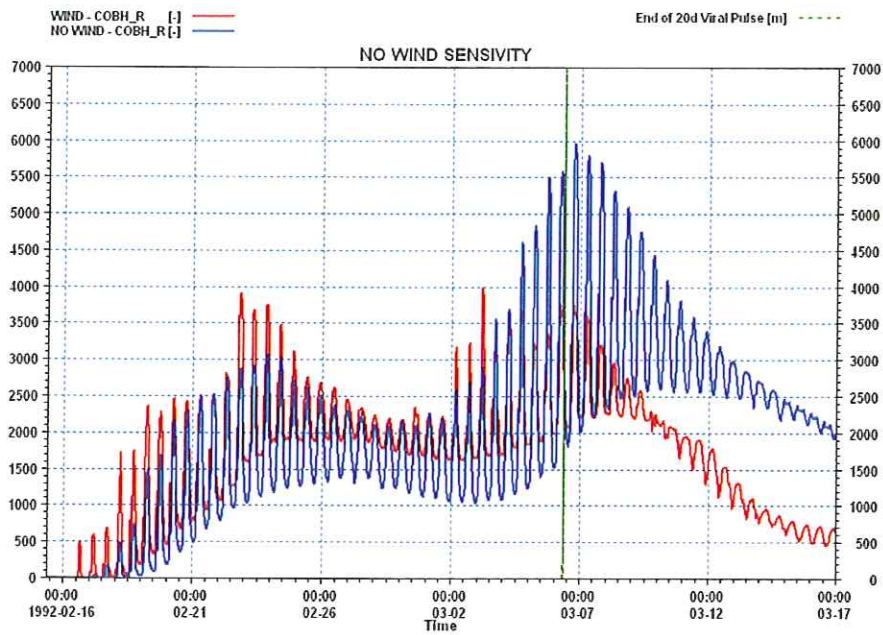


Fig. 7.19 No Wind Forcing Sensitivity – COBH\_R

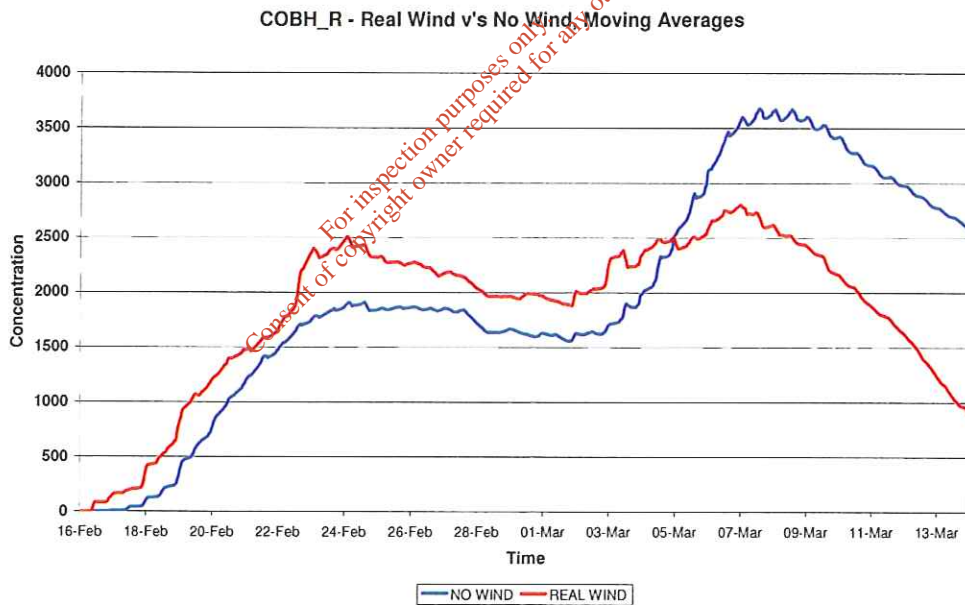


Fig. 7.20 Cobh\_R Moving Averages of Concentration for the wind sensitivity

From these plots we can see that the wind plays a major role in the contamination of the model oyster farm.

## 7.6 Sensitivity Five – Extremely Low River Flows in Summer

The results presented in Chapter 5 used the recorded river flows from February and March 1992. These flows were used for both the winter and summer conditions<sup>93</sup>. As part of the sensitivity analysis we have run the summer conditions for a number of the outfalls with extremely low river flows. Fig. 7.21 presents the results for CC\_S&C. In this figure the timeseries of concentrations for both cases are plotted on the left hand axis while both of the river flow timeseries are plotted on the secondary y-axis. The black dashed line is the River Lee flow timeseries for the results presented in Chapter 5 while the pink line is the River Lee flow timeseries for this sensitivity. We can see from the figure that there is a significant reduction in the contribution of CC\_S&C for this case.

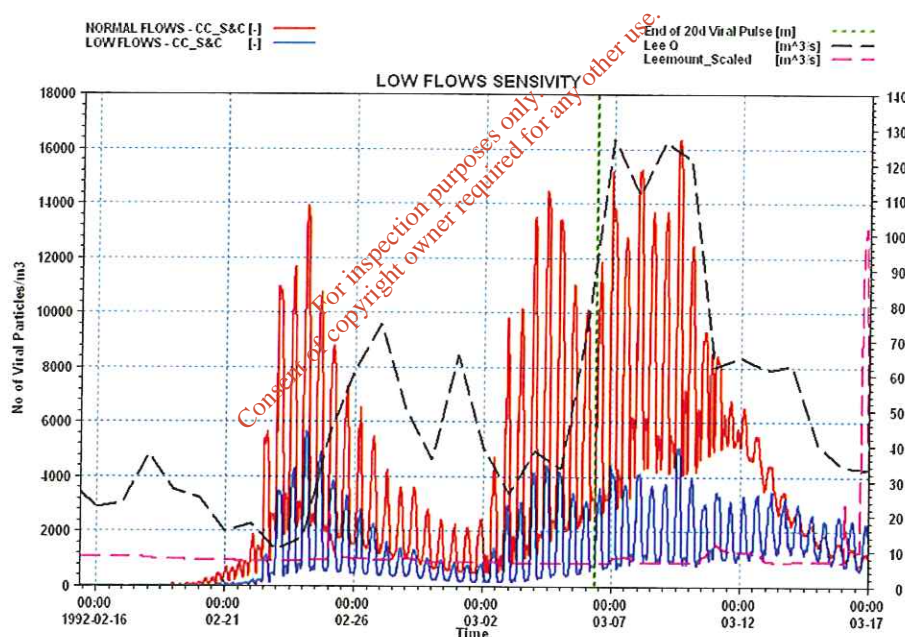


Fig. 7.21 Low Flows in Summer Sensitivity – CC\_S&C. The river flows are plotted on the secondary right axis

These reduced river flows need to be considered in the context of a year's data. Fig. 7.22 presents the recorded river flow from the gauge downstream of

<sup>93</sup> The gauge at Leemount failed for the first few months of 1992. The daily averaged flow from Inishcarra Dam, scaled to the correct catchment size at the Waterworks weir was therefore used.

Leemount Bridge. The low flows at the start of June were the flows selected for the sensitivity analysis in this section. We can see from the figure that much higher flows occur in summer and in the rest of the year. A three week period from this timeseries is plotted in Fig. 7.23. We can see quite clearly from this plot the influence which the dam at Inishcarra exerts on the flow in the River Lee. The rapid increase in flow is due to the sudden release of water from the dam which happens quite frequently. We can see from the plots that the flow at Leemount regularly exceeds  $80\text{m}^3/\text{sec}$  in both summer and winter.

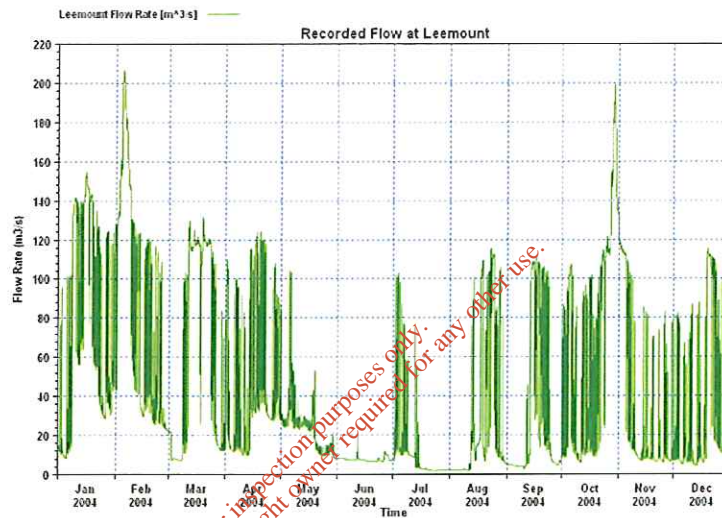


Fig. 7.22 Recorded Flow at Leemount Bridge – 2004

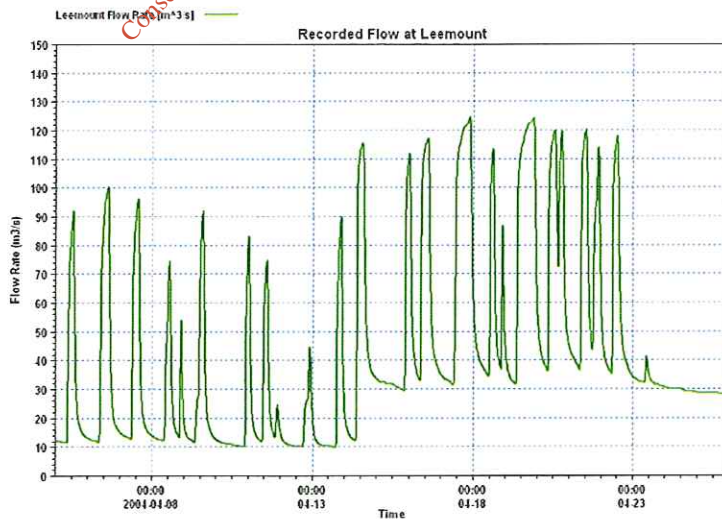


Fig. 7.23 Recorded Flow at Leemount Bridge – Detailed Period

The low flows sensitivity for RC\_S&C, CG and COBH\_ R are presented in the next three graphs. We can see from the figures that the contribution of these outfalls is not very sensitive to the low flows in summer.

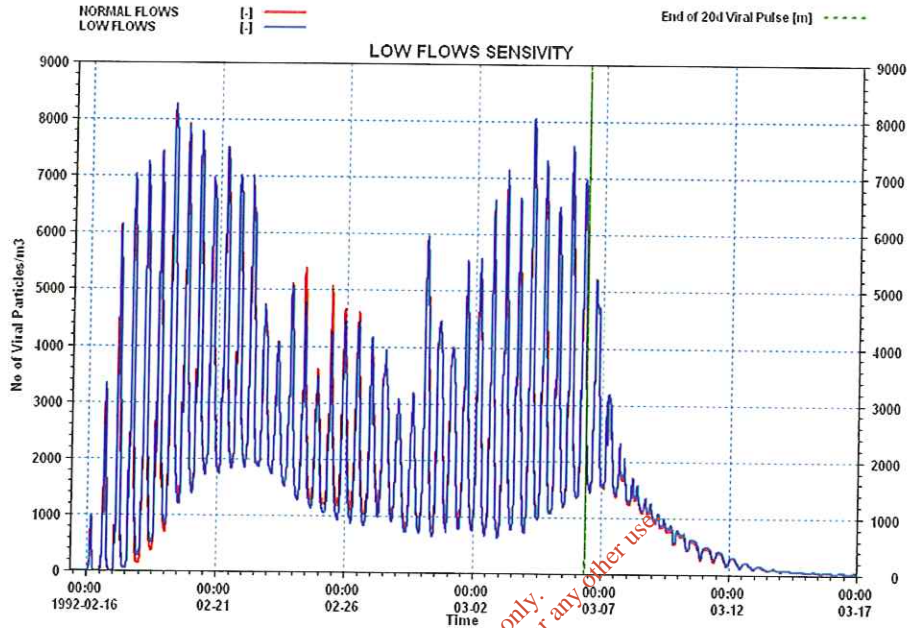


Fig. 7.24 Low Flows Sensitivity – RC\_S&C

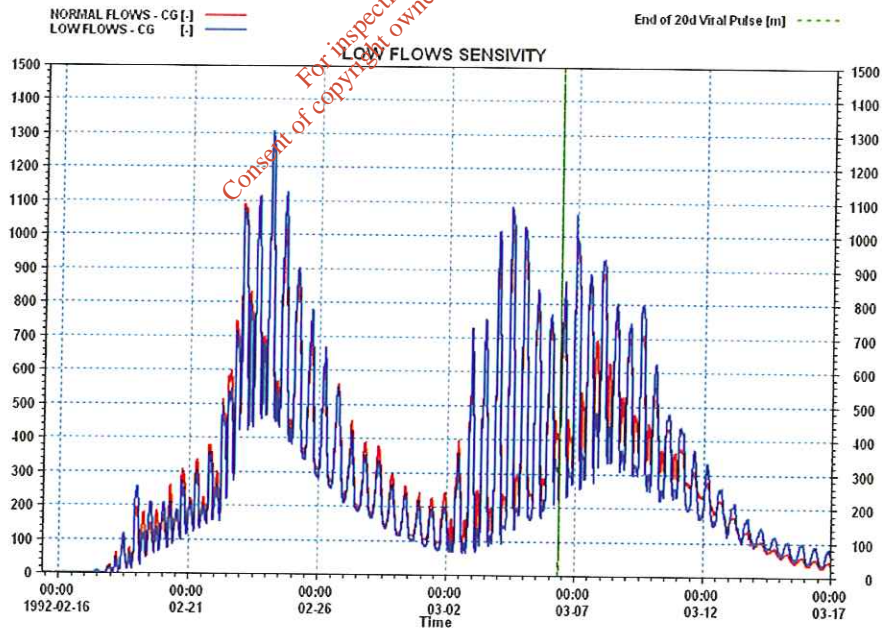


Fig. 7.25 Low Flows Sensitivity – Carrigrennan

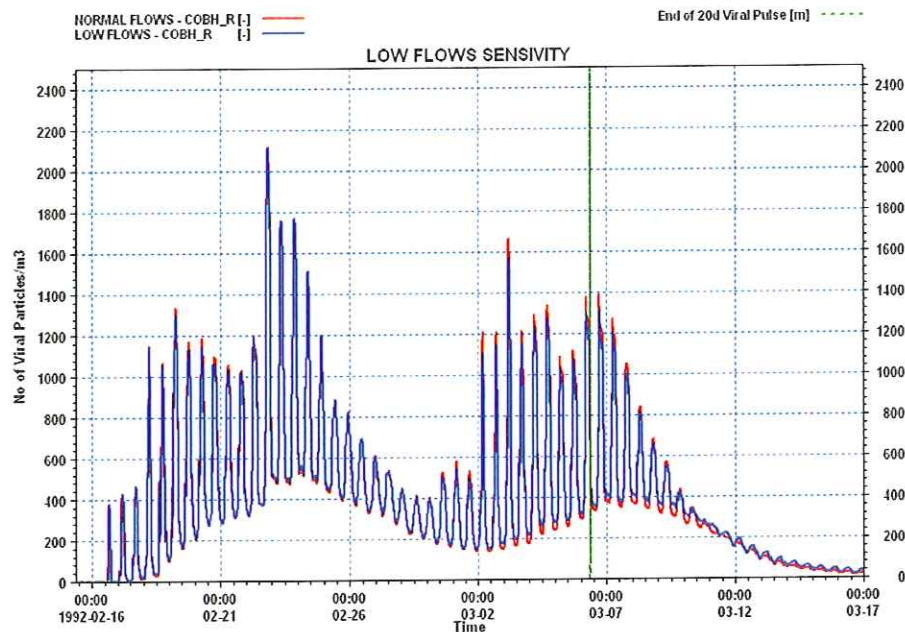


Fig. 7.26 Low Flows Sensitivity – COBH\_R

## 7.7 Sensitivity Six – Division of CC\_S&C

Before the construction of Carrigrohane the untreated waste from Cork City was discharged from a number of outfalls into Cork Harbour. The main outfalls serving the City were located at Horgans Quay and Kennedy Quay near City Hall. A number of other minor outfalls were located around the central island of the City, Blackrock village, Horgans Quay and Water Street. As well as these, separate outfalls served the Tramore Valley catchment and the Little Island/Glounthane catchment.

The results presented in Chapter 5 for the untreated waste from Cork considered each of these individual source discharge points to be discharged from a single outfall downstream of Horgans and Kennedy quay.

As part of the sensitivity analysis we have divided the sewage discharge into the three separate catchments: Cork City, Tramore Valley and Little Island/Glounthane. The Kennedy Quay outfall serving Cork City was moved a small distance upstream to the nose of the Central Island of Cork City. In the previous chapters this outfall had been placed just downstream of Kennedy Quay. The 1992 Main Drainage Report from EG Pettit Ltd allocates the sewer



catchments of Cork City to the main outfalls at Kennedy Quay, Albert Quay, Tramore Valley and Lough Mahon.

The difference between these two approaches is presented for the winter and summer cases in the following two diagrams. We can see from the figures that in both cases the differences are very minor. There are marginally higher peaks for the case when all the waste is discharged through a single outfall just downstream of Kennedy Quay.

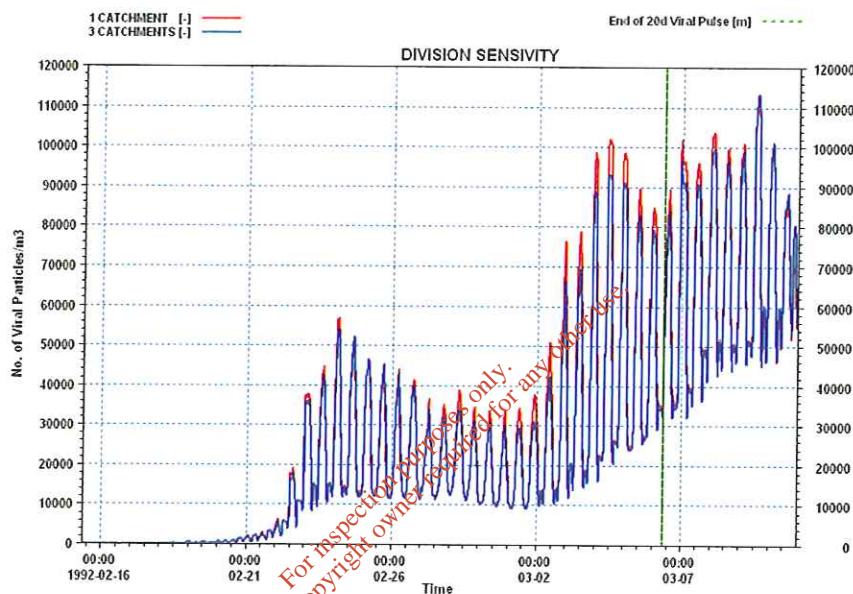


Fig. 7.27 Division of CC\_S&C into 3 catchments –WINTER

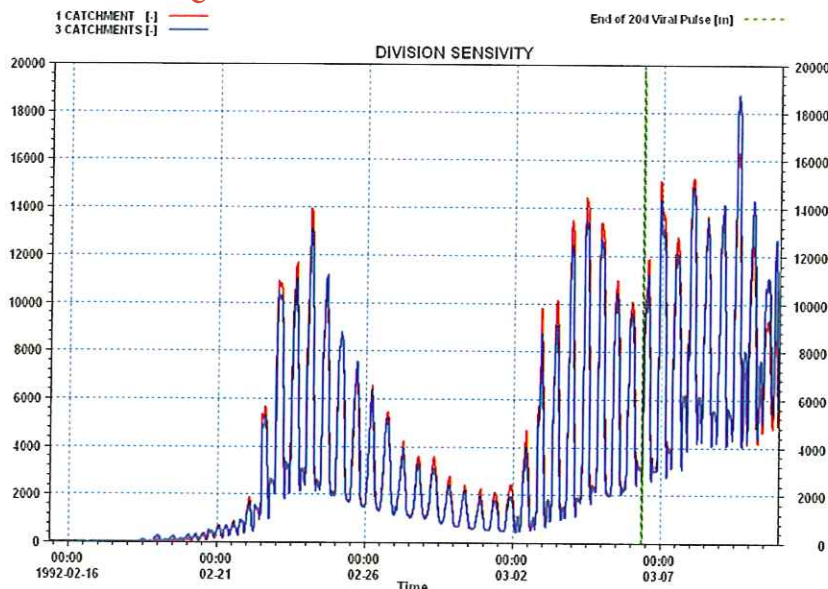


Fig. 7.28 Division of CC\_S&C into 3 catchments –SUMMER

### 7.8 Sensitivity Seven – Including Salinity, Winter Conditions

Salinity may be included in the model through the use of the ‘HD feedback’ option in the Advection dispersion model. When this option is included the horizontal density gradients become an additional forcing function in the momentum balance of the hydrodynamic model. Salinity has been included in the model as part of the sensitivity analysis.

Initial conditions, which describe the variation in salinity over Cork Harbour at a particular moment, may be estimated through the use of a regression equation<sup>94</sup> based on salinity measurements taken at high and low water at roughly seven two-monthly intervals during one year (Fig. 7.29).

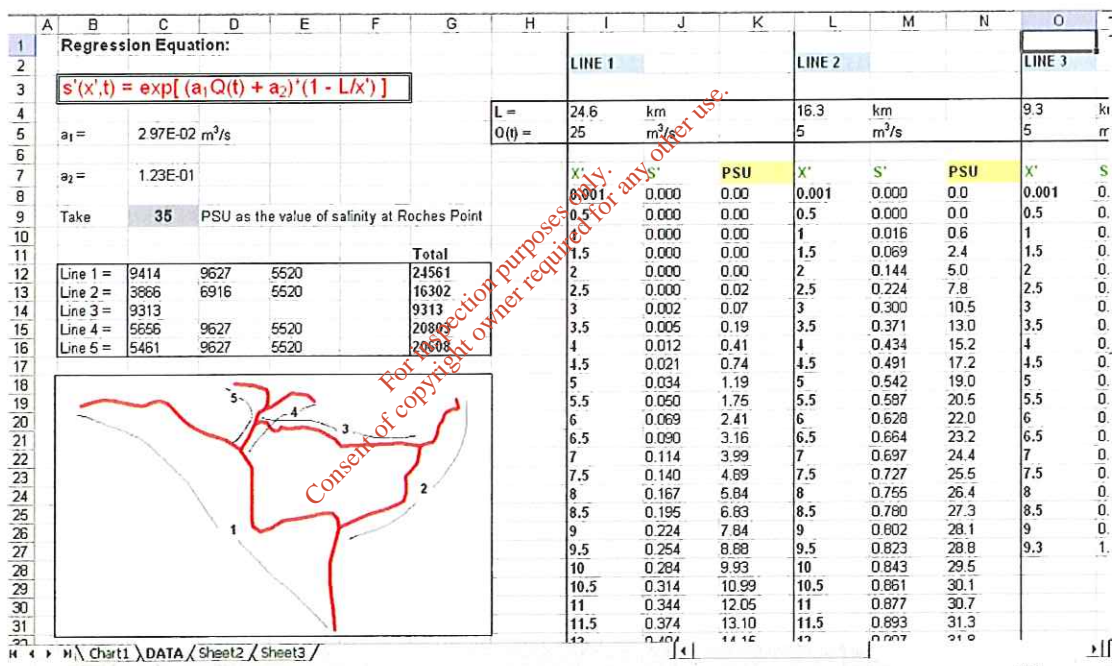


Fig. 7.29 Regression equation in excel

Using this regression equation, initial conditions, which describe the variation in salinity over Cork Harbour, were obtained. A two-week warm up period was then simulated with these initial conditions to allow for salinity and recorded river flows

<sup>94</sup> See Chapter 4 in O’Kane, JPJ “Estuarine Water Quality Management with moving element models and optimisation techniques” Pitman, London. 1980.

to interact. A constant value of 35psu was used as the boundary condition for the salinity.

The end of this two-week warm up period was chosen to coincide with the start of the 20 day viral pulse, 9:00am on the 15<sup>th</sup> of February.

The results from this sensitivity are presented in the following figures. We can see from Fig. 7.30 that the contribution of CC\_S&C at the centre of the model oyster farm has doubled. If we look at the moving averages (Fig. 7.31) we can see that this factor of two is consistent for the entire simulation period with the exception of the last day. We can see from Fig. 7.32 that the inclusion of salinity also doubles the contribution of Carrigrennan to the contamination of the model oyster farm.

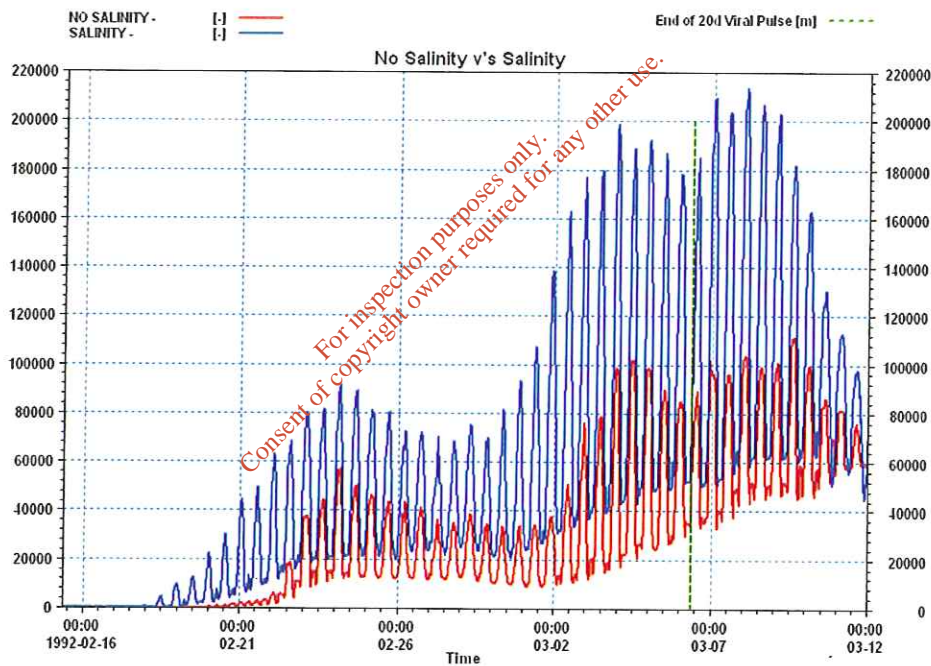


Fig. 7.30 Salinity Sensitivity – CC\_S&C

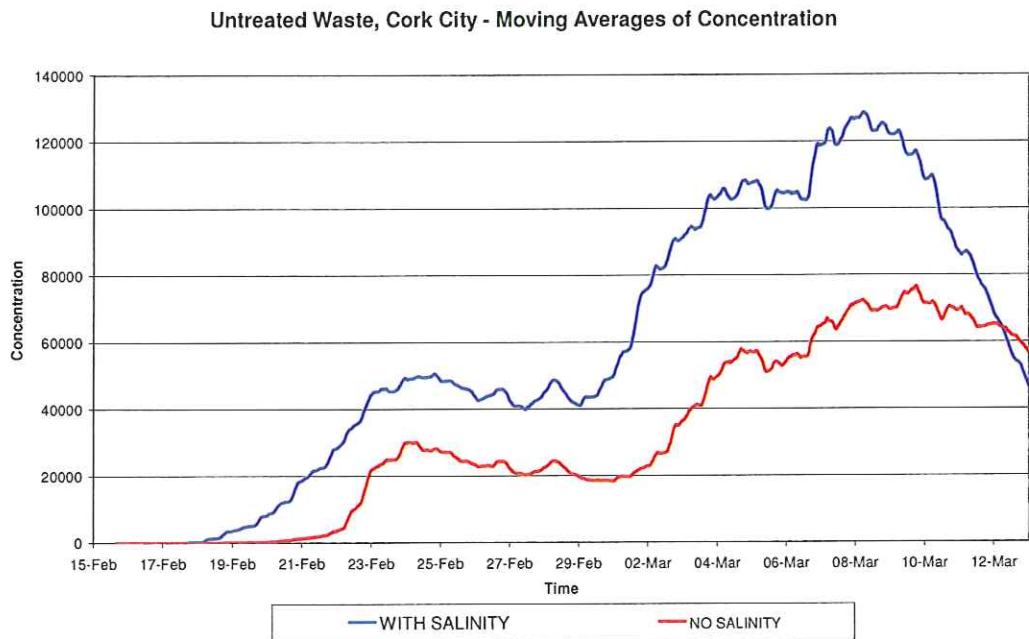


Fig. 7.31 Moving Averages – Salinity Sensitivity

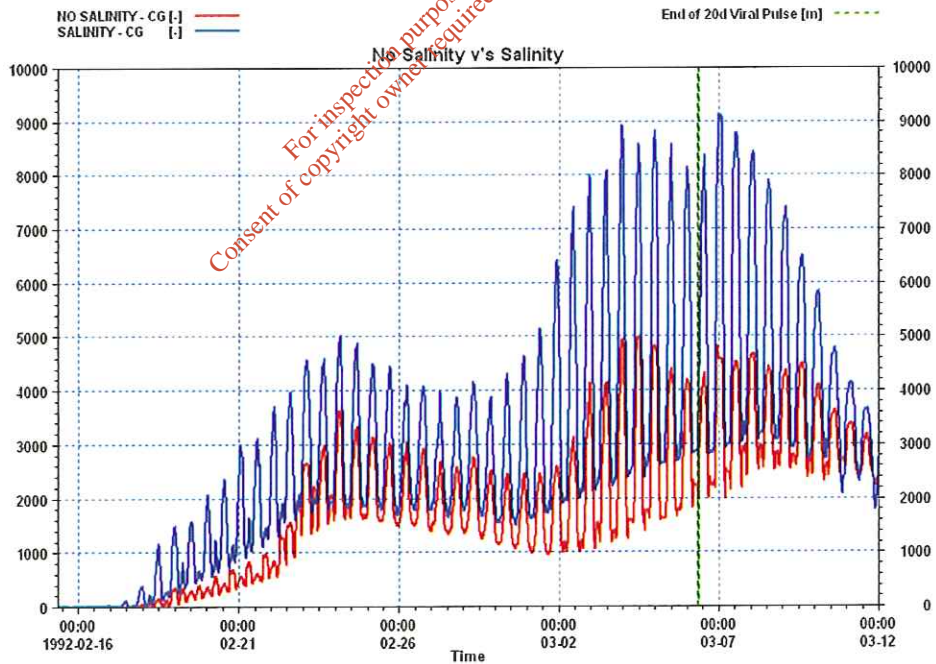


Fig. 7.32 Salinity Sensitivity – CG

If we look at COBH\_R (Fig. 7.33 and Fig. 7.34) we can see that there is also an increase. It varies between 10 – 30%.

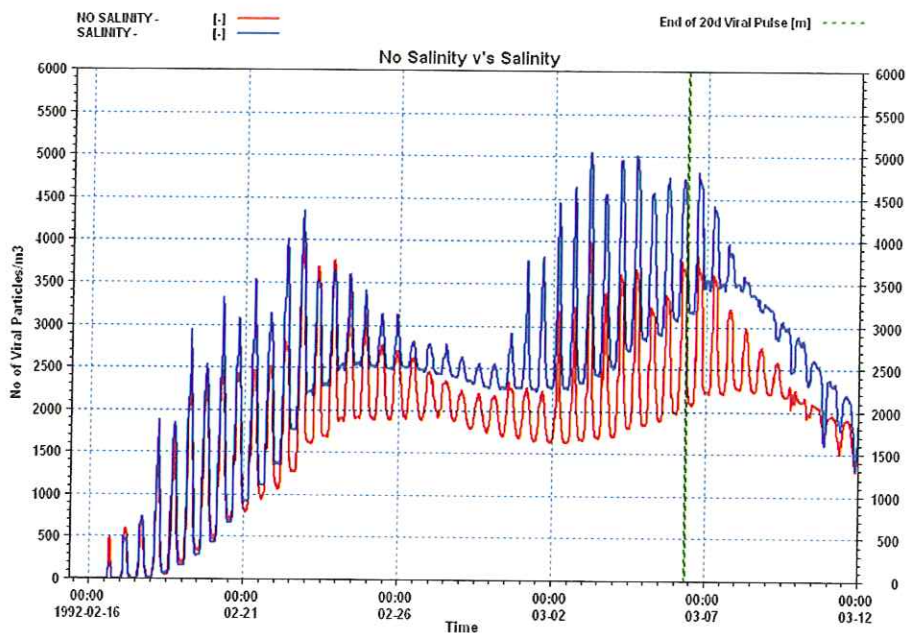


Fig. 7.33 Salinity Sensitivity – COBH\_R

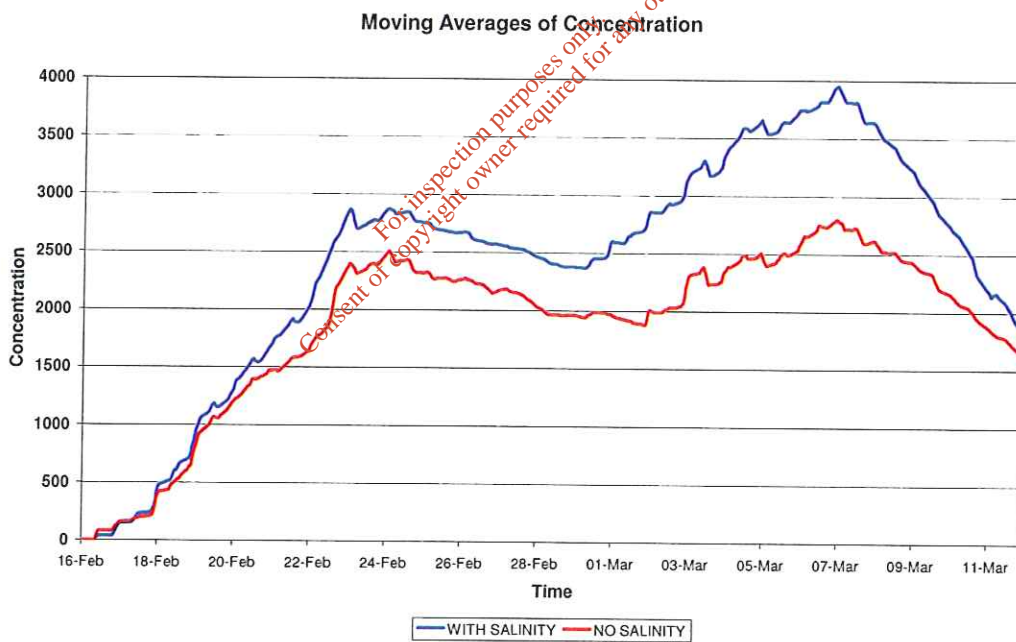


Fig. 7.34 COBH\_R – Moving Averages of Concentration

If we look at RC\_S&C however (Fig. 7.35 and Fig. 7.36) we can see that there is a minor change in the contribution of 5 - 10%.

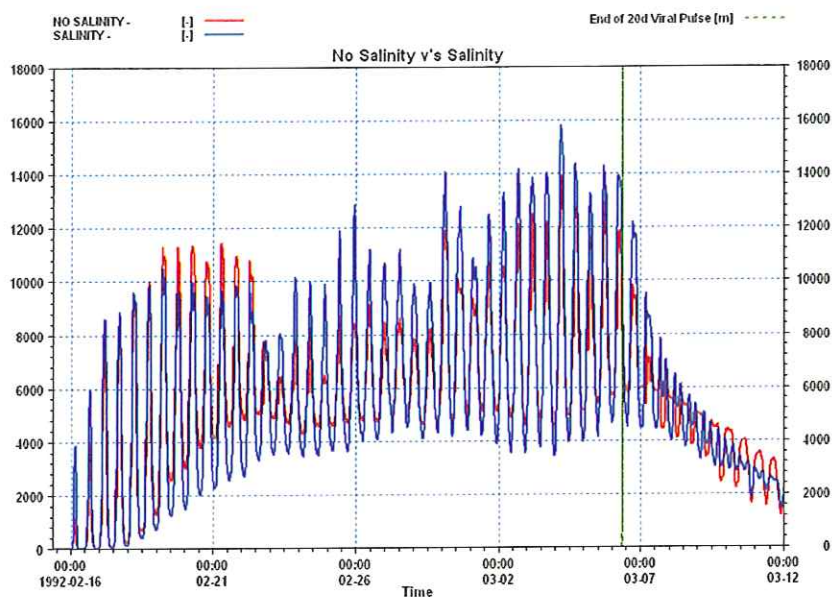


Fig. 7.35 Salinity Sensitivity – RC\_S&C

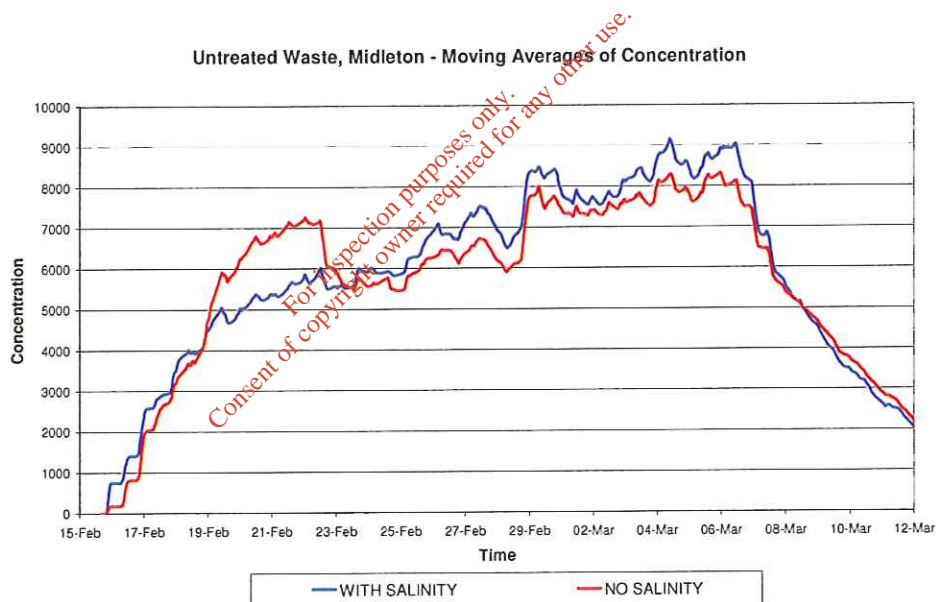


Fig. 7.36 RC\_S&C Moving Averages – Salinity Sensitivity

The results of the salinity sensitivity need to be treated with caution. No high-frequency measurements of salinity were recorded in the harbour and therefore no comparison of modelled salinity with recorded salinity can be made. As well as this we have assumed a constant value of 35psu<sup>95</sup> as the boundary condition

<sup>95</sup> <http://www.ria.ie/cgi-bin/ria/papers/100647.pdf>

of the salinity model. High-frequency measurements of salinity from Roches Point should be used to specify the boundary condition of a salinity model of Cork Harbour.

## 7.9 Examining different release patterns from Rathcoursey & a comparison between releasing Midleton's viral loading at Rathcoursey and at Bailick road in Midleton

As part of the sensitivity analysis we have examined different release patterns from the outfall at Rathcoursey. We have also made a comparison between the Rathcoursey and Midleton (Bailick road) discharge points by applying the loading from Midleton at each location under the same environmental conditions (no wind & no salinity) and comparing the resulting contamination at the model oyster farm.

### 7.9.1 Different releases from Rathcoursey

The results in Chapter 5 modelled the release from Rathcoursey as a 3 hour pulse on the ebb tide which commenced 30 minutes after high water. In this sensitivity we have modelled the release from Rathcoursey in four different ways as listed below. In each case we have modelled winter conditions ( $T_{90} = 30d$ ) for Period 1 (i.e. before the WWTP at Midleton was constructed) for 20 days. In each case we have excluded the influence of wind and salinity.

- SA\_1 – RC Pulsed on the ebb tide for 3 hours (same release as presented in Chapter 5)
- SA\_2 – Continuous release. There is a constant discharge of *Norovirus* from the Rathcoursey outfall on the ebb and flood tide.

- SA\_3 – The waste is pulsed from the outfall 1.5 hours before high tide for 3 hours. This release pattern corresponds to the way in which comminuted sewage was released from 1988 to 1992<sup>96</sup>.
- SA\_4 – Worse case scenario pulsing. In this case the untreated waste is released 1 hour after low tide for 3 hours such that all of waste is carried into the North Channel on the flood tide. This is a hypothetical pulsed release.

In order to make a valid comparison between the different release patterns we have used the same loading for each case.

The concentrations from the centre of the model oyster farm are presented in Fig. 7.37 below. The moving averages are presented in Fig. 7.38.

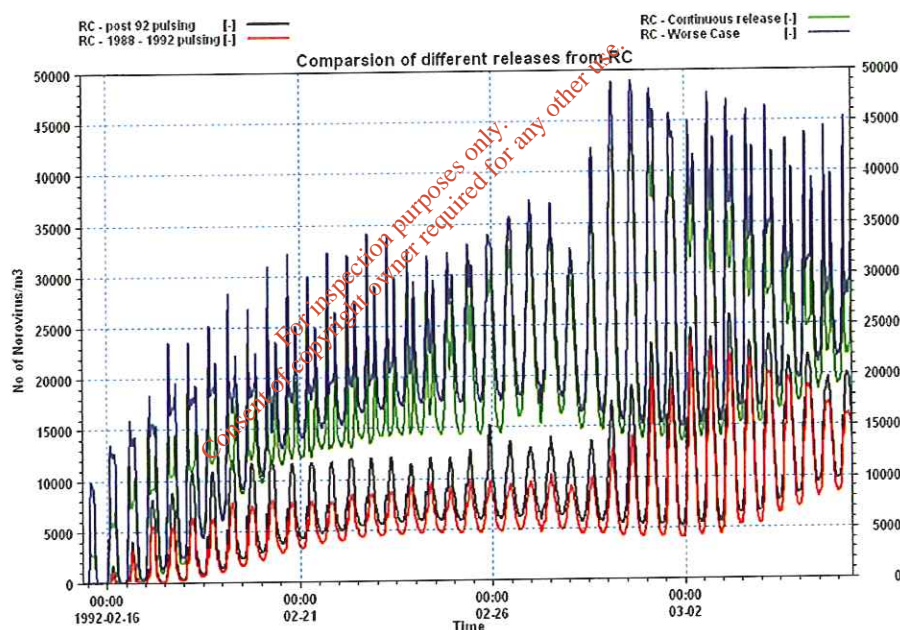


Fig. 7.37 Comparison of different release patterns from Rathcoursey

<sup>96</sup> Up to the middle of the 1980's there was no sewerage scheme in Midleton. Sewage was discharged to the estuary at various points within the town. Between 1986 and 1988, a new collection system was laid; comminuted sewage was now pumped to Rathcoursey and released on a tidal clock. From 1988 to 1992 the comminuted sewage was released 1.5 hours before high water for 3 hours. From 1992 onwards this was altered such that the comminuted sewage was released 30 minutes after high water for 3 hours.



We can see from Fig. 7.38 that when compared with the continuous release, the pulsing of the comminuted sewage reduced the contamination at the model oyster farm by as much as 50%. We can also see that the worse case pulsing scenario contributes more than twice the contamination of the post-1992 pulsing. We can also see from the figure that the pulsed release pattern from 1988 to 1992 is marginally better than the post-1992 pulsing.

The tidal clock at Rathcoursey is set manually on Monday every week for each day during the following period of two weeks. The resetting is required because the tidal cycle of 12 hours and 25 minutes is not synchronised with the day/night cycle of 24 hours.

If the clock were to continue to run without resetting the clock time of high water would diverge from actual time of occurrence by 50 minutes every 24 hours. After 6 days without resetting, the clock would say it is high water, when in fact it is low water and vice versa. In these circumstances the pulsed discharge would take place after low water directing the effluent inwards towards the oyster farm and not away from it. Consequently, the weekly setting and daily operation of the tidal clock should be subject to automatic audit. At present no records are maintained of its operation.

From the results presented in this sensitivity analysis we can see that the intended or design pulsing of the discharges from Rathcoursey has a beneficial effect on contamination of the model oyster farm.

In the sensitivity analyses SA1 to SA4, we have considered the untreated load from Midleton i.e. period 1. All releases from Rathcoursey in Period 3 and at present are treated with 95% removal of *Norovirus*.

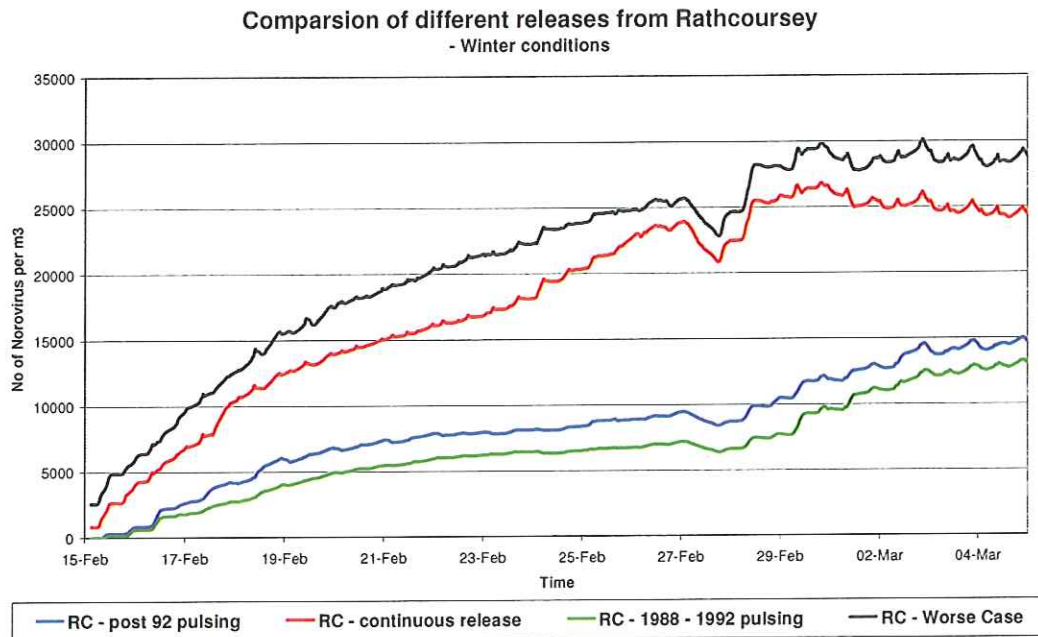


Fig. 7.38 Comparison of different release patterns from Rathcoursey – Moving Averages

### 7.9.2 Comparison between a *Norovirus* (T90 = 30days) release at Bailick road in Midleton and Rathcoursey

In order to make a comparison between a release of *Norovirus* at Rathcoursey and at Bailick Road in Midleton we have applied the untreated Midleton load at (a) Rathcoursey and (b) Bailick Road in Midleton<sup>97</sup>. We have modelled the release from Bailick road as a (1) continuous discharge and (2) pulsed discharge. The pulse is equivalent to the post 1992 discharge i.e. released for 3 hours 30 minutes after high water. Salinity and wind have been omitted from this sensitivity analysis. The two different sensitivity analysis runs are given as:

- SA\_5 – Pulsed discharge at Bailick, untreated Midleton load
- SA\_6 - Continuous release at Bailick, untreated Midleton load

<sup>97</sup> The source discharge point in the model used to discharge the untreated waste at Bailick road is representative of the discharge of waste from Midleton pre-1988. The point also coincides with the discharge point for Bailick 1 as presented in Chapter 5.

Both cases are plotted in Fig. 7.39. We can see from the plot that the contamination at the centre of the oyster farm is equivalent for both the continuous and pulsed releases.

The contamination at the model oyster farm from the Midleton load released at Bailick Road and at Rathcoursey is plotted in Fig. 7.40. We can see from the plot that the contribution from Bailick road is significantly greater than that from Rathcoursey. The moving averages are shown in Fig. 7.41. From this we can see that the contribution from the loading released at Bailick Road is approximately double that of it being released from Rathcoursey. For the first three days however the opposite is true. We can see from the plot that the loading released from Rathcoursey is greater than the loading from Bailick road up until the 18<sup>th</sup> of February.

We can conclude that when pulsed on the ebb tide Rathcoursey offers a much better location in which to release waste compared to the releasing it at Bailick road (i.e. the pre-1988 release location). Initially however Rathcoursey contributes more than the equivalent loading from Midleton.

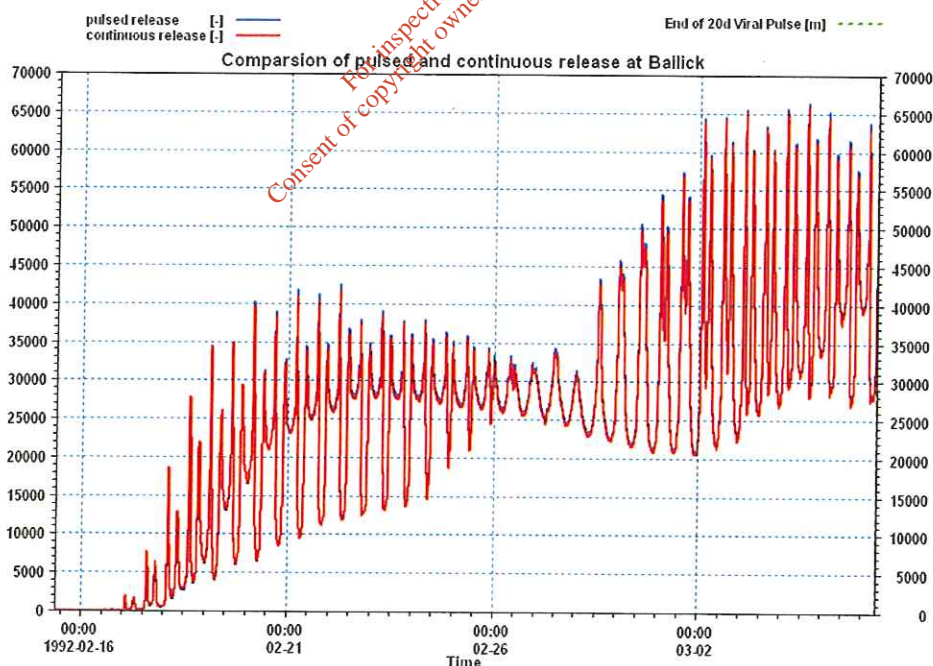


Fig. 7.39 Pulsed and Continuous release at Bailick Road

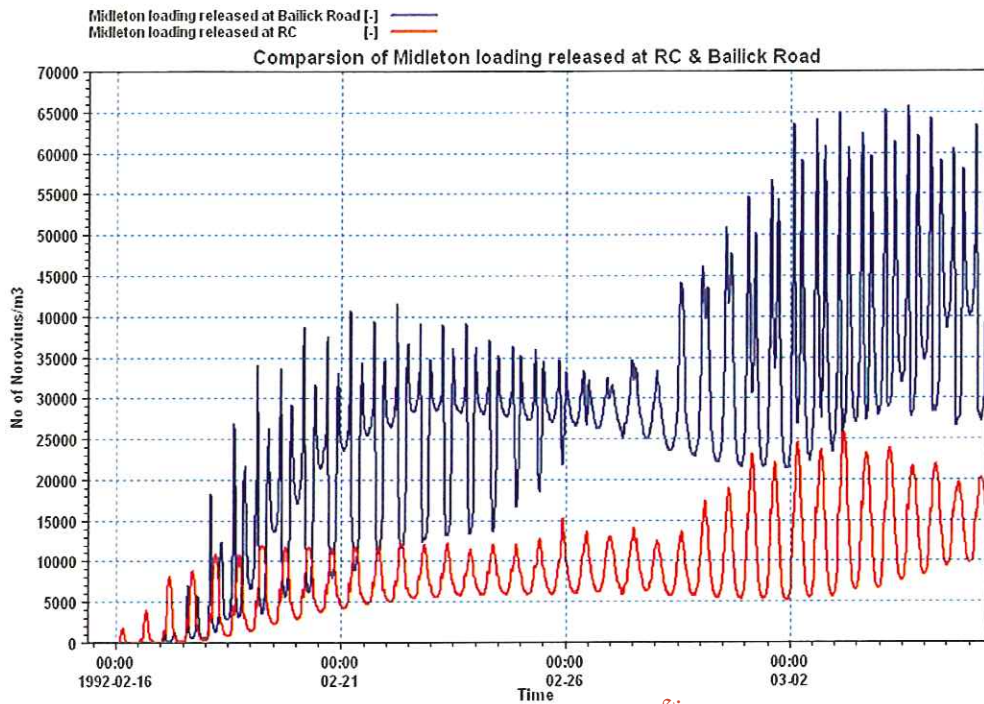


Fig. 7.40 Comparison of Midleton loading released at Rathcoursey and Bailick

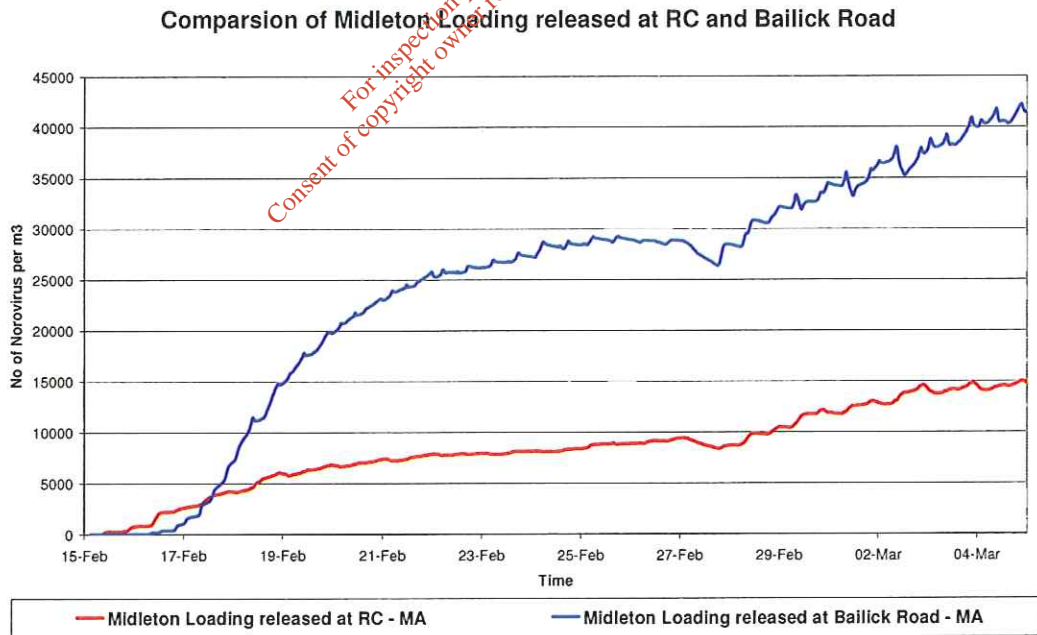


Fig. 7.41 Comparison between Rathcoursey and Bailick Road – Moving Averages

There are two main reasons why an identical viral load released at Bailick road and Rathcoursey differ in their contamination of the model oyster farm:

1. Although the outfall at Rathcoursey is closer than Bailick Road to the oyster farm, it is in effect further away because of the pulsing. The pulsed release of *Norovirus* ensures the plume is advected into the outer harbour on the ebb tide. On the ensuing flood tide the plume travels back up the East Passage and into the North Channel where it contaminates the model oyster farm. This combined distance is greater than the route from Bailick Road to the oyster farm (Fig. 7.42).
2. The *Norovirus* plume from Rathcoursey undergoes enhanced dilution and mixing in the greater volume of water in the outer harbour.

From this we may conclude that a pulsed release from Rathcoursey contaminates the model oyster farm to a lesser amount than an equivalent loading at released at Bailick Road in Midleton.



Fig. 7.42 Approximate path of Norovirus plume from Rathcoursey (Red Line – approximately 15km) and Midleton (Blue Line – approximately 6km).

The maximum and averaged concentrations for all the model runs considered in this section of the sensitivity analysis are presented in the following two figures. From both plots we can see that the contribution from the loading released at Bailick road is comparable to the contribution of the worse case scenario pulsing

from Rathcoursey. Consequently the weekly setting and operation of the tidal clock should be carried out in a fail-safe and verifiable manner.

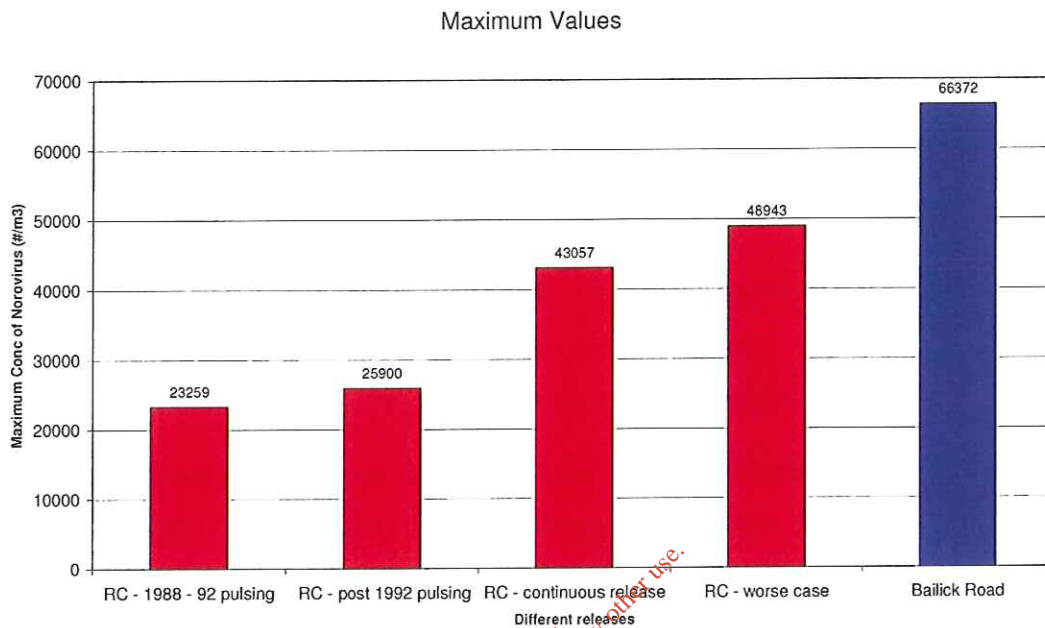


Fig. 7.43 Maximum values

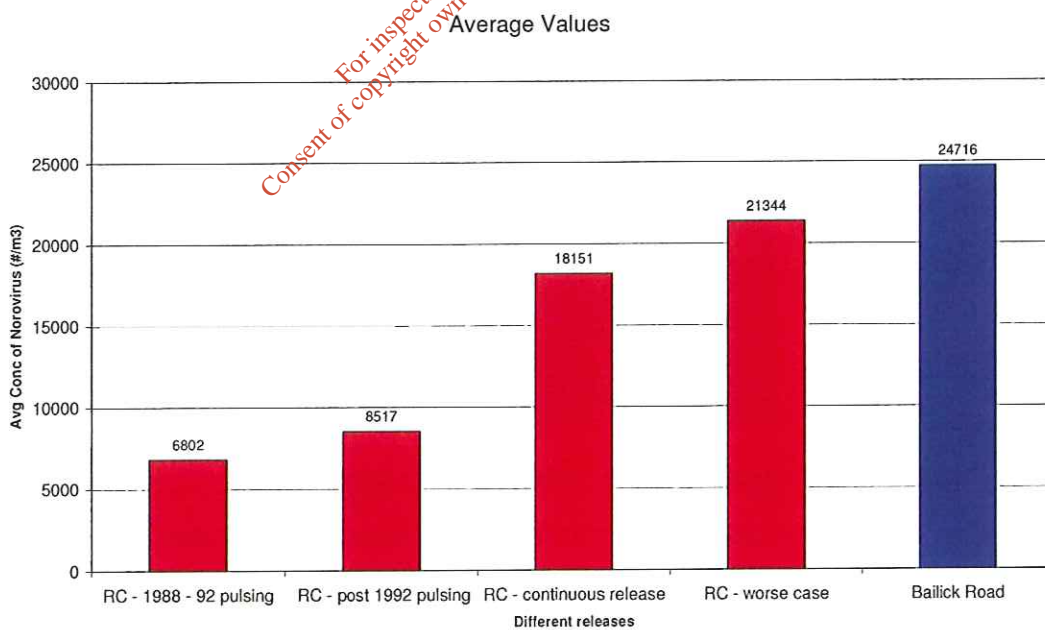


Fig. 7.44 Averaged values

## **7.10 Adsorption on suspended sediment**

When *Norovirus* is adsorbed on suspended sediment, discharges further away from the oyster farm may become less important because of possible sequestration of viruses in stationary bottom sediment; these processes are controlled by rates of sedimentation, resuspension, adsorption and desorption; insufficient data are available to make a secure model [qualitative statement].

For inspection purposes only.  
Consent of copyright owner required for any other use.

*For inspection purposes only.  
Consent of copyright owner required for any other use.*